Raman Spectroscopy of 2,4-DNT and its interation with sand particles

RAMAN SPECTROSCOPY OF 2,4-DNT AND ITS INTERATION WITH SAND PARTICLES

By

Alejandro Blanco Ocampo

A thesis submitted in partial fulfillment of the requirements for the degree of

MASTER OF SCIENCES
in
CHEMISTRY

UNIVERSITY OF PUERTO RICO
MAYAGÜEZ CAMPUS
2005

Approved by:

_____	_____
Nairmen Mina, PhD Member, Graduate Committee	Date
_____	_____
Miguel Castro, PhD Member, Graduate Committee	Date
_____	_____
Samuel P. Hernandez Rivera, Ph.D. President, Graduate Committee	Date
_____	_____
Narinder K. Mehta Ph.D. Representative of Graduate Studies	Date
_____	_____
María A. Aponte, Ph.D Chairperson of the Department	Date

ABSTRACT

Landmines have been a part of war technology for over 100 years. They are explosives charges that can be buried and then detonated by contact. Thousand of mines are currently placed on more than 70 countries all over the world. Up to now, metal detectors and other state-of the-art technologies have been used to detect these explosives devices. However, these techniques are incapable of detecting small quantities of explosives in solution and in small crystals. Raman Spectroscopy is an established tool for vibrational spectroscopy analysis and can be used in Point Detection mode to detect explosive components of landmines. Interactions of explosives with different substrates can be measured by using quantitative vibrational signal shift information of scattered Raman light associated with these interactions.

In this research, samples of 2,4-DNT were allowed to interact with sand samples. Characteristic vibrational signals of 2,4-DNT were analyzed in the ranges: 300-1200 cm^{-1}, 1200-1700 cm^{-1}, and 2800-3500 cm^{-1}. These variables were measured for 45 days. Raman Microscopy equipped with 514.5 nm laser excitation line was used. Sand samples doped with the nitroaromatic compound showed significant shifts in their Raman bands suggesting an interaction with the substrate. Samples of sand/2,4-DNT were analyzed acquiring Raman spectra at 9, 33 and 50% w/w of water and in the temperature range of

40-80 ^{o}C. Effect of pH on the mixtures was also studied in the range of 1-13. The mixtures were irradiated with ultraviolet light (254 nm) and Raman spectra were taken as a function of time.

High pH values and prolonged exposure to UV light of mixtures, alone and when mixtures were dosed with H_2O_2 showed extensive degradation as evidenced from the decrease of the intensities of the Raman signatures of the explosive. Exposure to heat at relatively high temperatures also resulted in partial degradation of DNT of the sand surface.

RESUMEN

Los explosivos han sido parte de la tecnología de guerra por más de 100 años. Son cargas de explosivos que se entierran y luego se detonan por contacto. En la actualidad miles de mines están sembradas en mas de 70 países alrededor del mundo. Actualmente detectores de metales y otras tecnologías modernas han sido utilizados para detectar estos explosivos. Sin embargo estas técnicas son incapaces de detectar cantidades pequeñas de explosivos en solución y en cristales. La Espectroscopia Raman es una herramienta utilizada en análisis de espectroscopia vibracional y se puede utilizar en la modalidad de Detección Puntual para detectar componentes explosivos en minas terrestres. La interacción de los explosivos con diferentes substratos puede medirse usando la señal vibracional del desplazamiento Raman asociada con estas interacciones.

En esta investigación muestras de 2,4-DNT se les dejó interactuar con muestras de arena. Las señales vibracionales características de 2,4-DNT fueron analizadas en los rangos: 300-1200 cm^{-1}, 1200-1800 cm^{-1} y 2800-3600 cm^{-1}. Estas variables fueron medidas durante 45 días usando un espectrómetro Raman acoplado a microscopio con un láser 514.5 nm. Muestras de arena dosificadas con el compuesto nitroaromático mostraron desplazamientos significativos en las bandas características que sugieren una interacción con el sustrato. Muestras de arena/2,4-DNT fueron analizadas tomándoles los espectros Raman con 9%, 33% y 50% w/w de agua y en un rango de temperatura de 40-80 ^{o}C. El efecto del pH en las mezclas se estudió en el intervalo de 1-13 de pH. Las

mezclas fueron irradiadas con luz ultravioleta (254 nm) y los espectros Raman fueron tomados en función del tiempo.

A valores de pH altos y exposición prolongada de las muestras a luz UV, solas o cuando se le añadió H_2O_2 a las mezclas, causaron degradación extensa según evidenciado por la disminución de las intensidades de las firmas Raman del explosivo. La exposición a calor a temperaturas relativamente altas también resultó en degradación parcial de DNT en la superficie de arena.

Table of Contents

Table of Figures

List of Tables

Chapter 1
Introduction

Landmines have been a part of war technology for over 100 years. They contain explosives charges that can be buried and then detonated by contact/pressure. Hundreds of mines are currently placed in more than 70 countries all over the world [Brannon, 2002]. Up to recent times, metal detectors and other state-of-the-art technologies have been used to detect these explosive devices [Yinon, 2002]. Antipersonnel mines remain a significant international threat to civilians despite recent intense efforts by the United States, other developed countries and humanitarian aid organizations to clear them from post conflict regions [Nolan et al, 1977]. Mines claim estimated 15,000–20,000 victims per year in some 90 countries. They jeopardize the resumption of normal activities; from subsistence farming to commercial enterprise, long after periods of conflict have ceased. For example, in Afghanistan during 2000, mines claimed 150–300 victims per month, half of them children [Bruschini, 1999]. Although most of these mines were emplaced during the Soviet occupation of Afghanistan (from 1979 to 1988), they continue to pose a serious risk to returning refugees and have placed vast tracts of farmland off limits. The United States currently invests about $100 million annually in humanitarian mine clearance, the largest commitment of any country. Despite this investment and the funding from many other developed nations and nongovernmental organizations, at the current rate clearing all existing mines could take 450–500 years, to do a full clearing job.

1.1 Limitations of Conventional Mine Detection Technologies

The tools available to mine detection teams today largely resemble those used during World War II. A deminer is equipped with a handheld metal detector and a prodding device, such as a pointed stick or screwdriver [Fisher et al. 2000]. The demining crew first clears a mined area of vegetation and then divides it into lanes of about a meter wide. A deminer then slowly advances down each lane while swinging the metal detector low to the ground. When the detector signals the presence of an anomaly, a second deminer probes the suspected area to determine whether it contains a buried mine. The overwhelming limitation of the conventional process is that the metal detector finds every piece of metal scrap, without providing information about whether the item is indeed a mine. For example, of approximately 200 million items excavated during humanitarian demining in Cambodia between 1992 and 1998, only about 500,000 items (less than 0.3 percent) were antipersonnel mines or other explosive devices. The large number of false alarms makes humanitarian mine detection a slow, dangerous, and expensive process.

Every buried item signaled by the detector must be investigated manually. Prodding with too much force or failure to confirm the presence of a mine during probing can lead to serious injury or death. Adjusting a conventional detector to reduce the false alarm rate results in a simultaneous decrease in the probability of finding a mine, meaning more mines will be left behind when the demining operation is completed. For humanitarian demining, trading off reductions in false alarms for reductions in the likelihood of finding buried mines is unacceptable. [Bruschini, 1999]

1.2 Capabilities of Innovative Mine Detection Technologies

Research is under way to develop new detection methods that search for characteristics other than metal content. The aim of these methods is to substantially reduce the false alarm rate while maintaining a high probability of detection, thereby saving time and reducing the chance of injury to the deminer. [Jacqueline, 2003]

For example, nuclear quadrupole resonance can find mines containing the explosive cyclotrimethylenenitramine (known as Royal Demolition Explosive [RDX]) with fast response time, but it is slow in confirming the presence of trinitrotoluene (TNT). Acoustic mine detection systems have demonstrated very low false alarm rates, but they cannot find mines buried at depths greater than about one mine. Chemical vapor sensors can find plastic case of mines in moist soils, but they have difficulty locating metal case mines in dry environments [Gupta, 2000].

Given the limitations of individual sensor technologies, major breakthroughs in mine detection capability are likely to occur only with the development of a multi sensor system. However, most of these techniques are incapable of detecting small quantities of explosives in solution and in small crystals.

Various sensor-based techniques for landmine detection and clearance have recently been reviewed. These techniques exploit different properties (e.g., thermal, chemical). An ideal sensor would be able to detect the actual explosive material (e.g. TNT, DNT and RDX) rather than detect parts used in the construction of the landmine. Sensor can be based on vibrational spectroscopy, laser absorption etc. [Katrin et al, 1999]

Raman spectroscopy (inelastic light scattering) complements IR spectroscopy as a method for obtaining vibrational information about molecular species. While Raman

spectra are available for most explosive materials of interest [Gupta, 2000], it is only recently that this method has emerged as a promising tool for trace level detection. Raman spectroscopy is a well-established technique for analyzing and identifying materials and can be applied to the identification of explosives in the field, and to design sensors based on inelastic scattering.

1.3 Explosives

Explosives are substances that have been used for a long time. An explosive is a compound or mixture used to release, by a chemical reaction, considerable amounts of energy in a confined space and so rapidly that mechanical movement or shattering of surroundings objects is obtained [Akhavan, 1998]. Ancient Asian alchemists accidentally made the first explosive more than two thousand years ago [Federoff 1980]. By mistake they mixed saltpeter and sulfur, and did not add coal, before mixing addiction of coal after heating the mixture to detonate to rise to an explosion. Their invention was not used for war; instead, it was employed for communication. Later the Asians using their explosive technology developed a crude projectile weapon, and then the Arabs stole the Asian’s knowledge and used it for war. From that moment the age of the explosives had begun.

The explosives can be classified by their performance and uses: Primary explosives (low explosives) undergo a very rapid transition from burning to detonation. They can transmit the detonation to less sensitive explosives. They can be detonated by heat or shock. Example of a primary explosive is mercury fulminate and lead azide..

Secondary explosives (high explosives) cannot be detonated readily by heat or shock, and they are less sensitive than primary explosives, so they need the later to detonate. Examples of secondary explosives are: DNT, TNT and RDX. Dinitrotoluene (DNT) is one of the high explosives that have been used for military purposes since 1902 [Colling 1999].

Propellants only burn and do not explode under ordinary conditions. They can be initiated by a flame or spark. Examples of propellants are: black powder, ammonium nitrate and double bases.

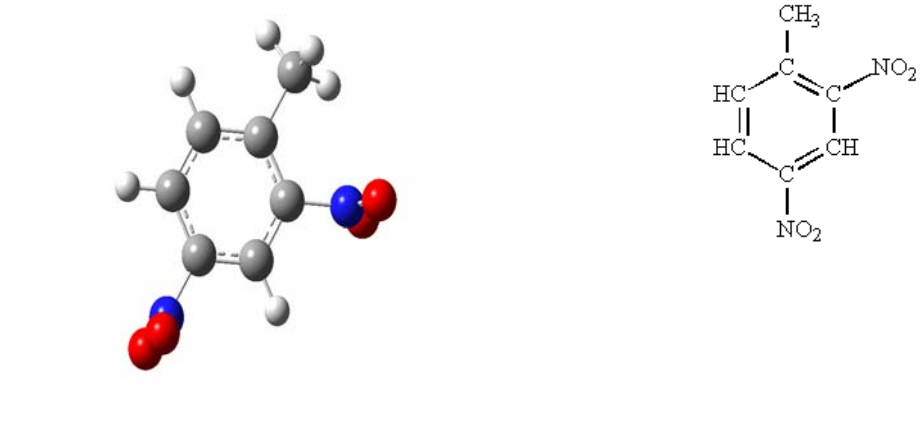

Figure 1.1 2,4-DNT chemical structure.

DNT shown in Figure 1.1 is one of the most common explosives found in landmines. It occurs in approximately 80 per cent of all mines [George et al, 1999]. Explosives that are based on TNT contain by-products, primarily impurities and degradation products such as DNB (Dinitrobenzene) and DNT [Buttner et al, 1999]. DNT is one of the main explosives used in the production of landmines and is a product of degradation and an impurity in the synthesis of TNT [Kenna et al, 1986].

Some of the explosives that that constitute secondary components of landmines are 1-methyl-2, 4 dinitrobenzene, and 1-methyl-2, 6 dinitrobenzene better known as 2,4 and 2,6-DNT. These two compounds are manufactured by dinitration of toluene or by mononotration of p-nitrotoluene. Mononitration of o-nitrotoluene leads to a 1:2 mixture of 2,4 and 2,6-DNT [Glenn et al, 2002]. When explosives come in contact with soil, humidity, at various pH and under the action of UV radiation they experiment reactions that change the characteristic signatures [Yinon, 1999].

Table 1.1 Full Screening Information Data Sets (SIDS) of 2,4-DNT.

Synonyms	2,4-Dinitrotoluene, Benzene, 1-methyl-2,4-dinitro, 2,4-DNT
Molecular Formula	$C_7H_6N_2O_4$
Apparent Color	Yellow needles or monoclinic prisms
Boiling Point	300 ^{o}C with slight decomposition
Molecular Weight	182.14
Melting Point	71 ^{o}C
Density	1.3208 g/ml to 71 ^{o}C
Boiling Point	319.5 °C (at kPa)
Vapour Pressure	7.9.10-6 kPa at room temperature
Water solubility	166 mg/l at °C
Odor	slight odor

1.4 Objective

The main objective of this research was to characterize the vibrational Raman signatures of 2,4-DNT. These signatures were studied in solution, transferring onto metal surface in formation of solids (amorphous and crystalline) and in neat crystals. The second objective of this work was the detection and a spectroscopic signature study of 2,4-DNT in mixtures with sand particles in different proportions of sand/DNT. As a last objective, it was of interest to find the effect of pH, humidity, UV light exposition and temperature in the interaction of 2,4-DNT and these sand particles.

Chapter 2
Previous Works

Sylvia, and collaborators [Sylvia, 2000], demonstrated the capabilities of Surface Enhanced Raman Spectroscopy to detect the chemical vapor signature emanated from buried TNT-based landmines. They presented reproducible results from blind tests controlled by the Defense Advanced Research Projects Agency (DARPA) that demonstrated vapor detection of 2,4-Dinitrotoluene at concentration levels of 5 ppb or less. The authors used acquisition times 30 s using a fieldable system and showed that SERS can represent a significant improvement over current landmines detection methods.

Buttner, showed the progress made in the development of rapid method for locating and quantifying explosives and byproduct contamination soils. Insoluble explosives solids tend to exist heterogeneously distributed particles in soils, thus made it difficult to precisely define concentration levels. They developed an analytical system that can be installed in the limited space inside a cone penetrometer to measure subsurface contamination by explosives in soils. The principles of detection consist of three steps, (a) vaporization of explosive, (b) thermal decomposition of the vapor to simpler compounds and (c) measurement of nitrogen oxides on miniature amperometric sensors [Buttner 1997].

The thermal decomposition of 2,4,6-TNT, RDX, HMX and other explosives over heated noble metal surfaces generates characteristic products that can be detected by amperometric gas. This observation was exploited to develop a method for the selective *in situ* detection and quantization of explosives contamination in soils. Amperometric

sensing of the compounds generated from the thermal decomposition of soil bound TNT was selective and sensitive over broad range a field test demonstrated that this method is viable for *in situ* analysis of explosives.

Lewis obtained the Fourier Transform (FT)-Raman spectra of 32 explosive materials [Lewis, et al, 1997]. Twenty-eight of the explosives were categorized into three classes: nitrate esters, nitro aromatics, and nitramines, based on their chemical structure, the position of the asymmetric and symmetric stretching vibrations of the nitro group, and the shapes of the bands envelopes. The other explosives remaining were classified as exceptional explosives due to, their unusual structures or compositions that resulted in non-conventional Raman spectra. An example of this was the spectra obtained for 1,3,5-triamino-2,4,6-trinitrobenzene (TATB) and Semtex. Three mayor classes of explosives: the nitrate esters containing the R-O-NO_2 group, the nitro-aromatic containing the Ar-NO_2 group and the nitramines containing the R-N-(NO_2) group could be distinguished on the basis of their Raman spectra. They found that for spectral classification of explosives, the intensity of the CH stretching vibrations and the positions of the nitro group vibrations are important when distinguishing nitrates esters and nitramines from nitro-aromatics. Also the symmetric NO_2 stretching vibration was the most intense band in most of the explosive materials studied. Exceptions included C-4, HMX, RDX, TATB, and TNN.

Gauger studied the reduction of nitro aromatic compounds which are widely used in agrochemicals and explosives. The method was based on a displacement immunoassay performed in a commercial instrument, the FAST 2000, engineered by Research International Inc. The method can be used on-site to measure TNT and RDX within 5

minutes. Statistical analyses were done to assess accuracy, bias and predictability of the method. The results demonstrated that the immunosensor could be used effectively to screen environmental samples for the presence or absence of explosives [Paul, 2001].

Naal and collaborators employed biological materials as sensing means for explosives. Among the numerous types of biosensors, amperometric biosensors have been among the most successful and seem very promising for a wide range of applications. The preparation and characterization of an amperometric TNT biosensor based on the surface immobilization of a maltose binding protein (MBP) nitroreductase (NR) fusion (MBP-NR) onto an electrode modified with an electro-polymerized film of N-(3 pyrrol-1-ylpropil)-4-4'-bipyridine. The MBP domain of MBP-NR exhibits a high and specific affinity towards electro-polymerized films of MPB with the immobilized enzyme retaining virtually all of its enzymatic activity. The kinetics of the catalytic reaction between the biosensors and TNT and 2,4-DNT was characterized using rotating disk electrode and cyclic voltametry techniques. The limits of detection for both TNT and 2,4-DNT were estimated to be 2 μM and the sensitivities were determined to be 205 and 222 nA/μM, respectively [Naal, 2002].

Chapter 3
Raman Microspectroscopy

The Raman effect is an inelastic light-scattering phenomenon in winch the frequency of a monochromatic incident light illuminating a sample changes form v_o to another frequency v_1 [Ferraro 1994]. The frequency difference (v_o - $v_{1)}$ which may be either positive or negative, is generally called the Raman frequency or Raman Shift. The Raman effect arises when the incident light excites molecules in the sample which subsequently scatter the light. Most of the scattered light is at the same wavelength as the incident light (elastic or Rayleigh scattering). However, a small part of the scattered radiation can have a different wavelength. This inelastically scattered light is called Raman scattering. This frequency shift and the corresponding energy difference corresponds to a change in vibrational energy of a molecule. The difference in energy between the incident photon and the Raman scattered photon is equal to the energy of the vibration of the scattering molecule**.**

If the molecule loses energy during this process the scattered light is called Stokes radiation and if the molecule gains energy the radiation is called anti-Stokes. A plot of intensity of scattered light versus energy difference is a Raman spectrum. The concentration of the molecules in the samples can be determined by the intensities of the peaks.

The name of this phenomenon comes from the experimental discovery by C.V. Raman, who first observed this effect in spectrum of liquid benzene in 1928. In almost 80 years, Raman spectroscopy has been developed to become one of most powerful

techniques for the study of molecular structure and the principal method of non-destructive chemical analysis.

3.1 Raman Microscopy

The basic Raman instrument consists mainly of an excitation source, collection optics, monochromator and detection and recording system [McCreery, 2000]. The current excitation source use is a laser which has a filter to remove other lines, in order to make it truly monochromatic. Raman microscopy uses a microscope objective as the lens to focus the laser beam and to collect the scattered light in a 180° or backscattering mode. The monochromator normally disperses the Raman light and separates the Rayleigh scattering light from the Raman signal. The size of the sample and the focal spot are of the order of one to few microns. Raman Microscope is a hybrid of optical microscopy and Raman spectroscopy in consequence, has all the concomitant advantages of both techniques. The main purpose of the microscope is to excite, collect and couple the Raman radiation very efficiently from the sample to the spectrometer, and to provide a means for sample positioning and viewing at high magnification. [Clarke et al, 2000]

The Raman microscope can analyze the vibrational frequency shifts at different points on a surface. A Renishaw RM2000 Raman Microspectrometer was used to measure vibrational spectra of samples analyzed. This instrument performs two functions: first, the microscope takes Raman vibrational spectra of micron size samples. Second, the microscope produced 2D magnified images using the white light.

The Renishaw Raman Microspectrometer system consists of two main parts: on the right hand side has a spectrometer and an optical microscope on the left. The

instrument has two holographic notch filters (HNF), the first functioning as the combination of beam splitter and a rejection filter and the second purely as a rejection filter. The HNF is able to reject light at laser frequency by factors between 10^{-3} and 10^{-6} and transmit up to 80% of the light at other frequencies. The laser beam is directed onto the sample by mirrors, a beam collimator, by the first HNF and by the microscope objective.

The backscattered light at 180^{o} from the sample is collected by the same objective and fed back into the spectrometer. The two HNF block the Rayleigh scattered light and reflected light but the Raman scattered light is transmitted. To take Raman images the laser beam is defocused through the adjustment of the beam collimator to illuminate an area of the sample. Then the scattered light from this area forms the image. Two mirrors allow the instrument perform the Raman microprobe function. On the other hand, a filter wheel holder is used to house six dielectric narrow-band-pass filters that have different transmission bands are used to generate vibrational images. The filter transmission band centers is a function of the incident angle of the light and permit to cover spectral ranges from 100 cm^{-1} to 4000 cm^{-1}. The detector used was a CCD (charge-coupled device).

Chapter 4
Materials and Methods

4.1 Chemicals

Solutions of 2,4-DNT were prepared from Standard Solutions, 1000 µg/mL, 1.2 mL acetonitrile obtained from Cerilliant Corp., Round Rock, TX. Crystals of 2,4-DNT, containing a minimum 30% water were obtained from Chem Service Inc., West Chester, PA. Ottawa sand used was obtained from EM Science, Darmstadt, Germany. All of the standards were used as the acetonitrile (ACN) solutions and had an initial concentration of 1000 parts per million (ppm). HPLC grade methanol was supplied by Aldrich Chemical Co., Milwaukee, WI.

Stainless steel slides were also used to analyze the mixtures of explosive and sand particles. Gold coated micro-slides obtained from Spectra Tech Co., Madison, WI were used to measure Raman spectra of neat samples. Eppendorf pipettes, Brinkmann Instruments Inc., Westbury. NY, were used to prepare all solutions and for liquid sample transfer. Dispersive Raman Microscopes (785 and 514 nm) from Renishaw Instruments, Chicago, IL were used in Raman experiments.

4.2 Interacting mixtures of 2,4-DNTwith Ottawa Sand

Several mixtures of 2,4-DNT and Ottawa Sand were prepared. The samples were mixed using Vortex™ mixer during 5 minutes at 3000 rpm. The proportions used for the sand/DNT mixtures were 1:1,10:1, 100:1,1000:1, 10000:1, the spectra were taken and compared with pure crystalline sample of 2,4-DNT.

4.3 Effect of water and pH on Ottawa Sand/2,4-DNT mixtures

The effect of addition of quantities of water to Ottawa Sand/DNT mixtures was studied. Samples of mixtures were placed in cylindrical stainless steel cells (1 in. diameter, 0.25 in. high) and distilled water was added in different proportions of: 9%, 33%, and 50%w/w water. Raman spectra were taken before and after water addition.

To establish the effect of acid or alkaline pH, solutions of different pH from 3 to 12 were added to the mixture of the explosive and the sand particles. The pH at the solution was modified by adding acid or alkaline solutions to mixtures. Raman spectra were measured after the solvent evaporated. The obtained spectra were compared with the spectrum of neat crystals of 2,4-DNT.

4.4 Effect of temperature

The effect of heat was studied by exposing the samples to heat on an oven at fixed temperature. Several temperatures were studied to asses the effect on the mixtures between DNT and Ottawa Sand particles. The interaction of DNT/sand was placed in an oven varying the temperature from 40 ˚C to 90 ˚C. The spectra of the mixtures were taken after heating and cooling cycles in increments of 10º C. The resulting spectra were compared with the spectra of the near mixture components.

4.5 Effect of UV Radiation, Hydrogen peroxide and high pH

Mixtures of DNT/sand substrate were exposed to the effect UV radiation operated in long and short wave modes. Samples of pure DNT were also placed under the UV lamp to be used as reference. Spectra of all samples were obtained before UV exposure and every day for a period of 20 days on each mode to establish a comparison with the

Raman spectra for pure DNT. A UVP-Ultra-Violet Products bench top cabinet equipped with a UV lamp used. The UV source was a 6 watt C-15G lamp with short wave 254 nm and long wave 360 nm lines. Samples of DNT at pH = 10 and H_2O_2 were placed in the presence of ultraviolet light at 254 nm during 6 hours. Raman spectra were taken before and after UV radiation exposure.

4.6 Raman measurements

Renishaw Raman Microspectrometer RM2000 system was employed for the vibrational spectroscopy measurements. This system is equipped with a Leica microscope. The 514.5 nm laser line of a Coherent INNOVA 308 argon ion laser line was employed as excitation source. The laser beam was focused onto the samples through objectives with 5x, 10x, 20x and 50x magnifications. The Raman Shift spectra were obtained in the 100-3800 cm^{-1} range. An integration time of 10 seconds was used. Three acquisitions were averaged per scan in order to improve the signal to noise ratio. A nominal 1 cm^{-1} resolution was maintained in order to look for small changes in the Raman Shift spectra.

Chapter 5
Results and Discussion

The first objective of this investigation was to obtain Raman Spectroscopy baseline measurements of the vibrational signatures of the important nitro aromatic explosive 2,4-DNT. A difficulty was encountered when trying to obtain crystalline samples by micropipette transfer of acetonitrile standard solutions of 2,4-DNT: crystals were not readily formed from solvent evaporation but rather seemingly amorphous mass deposits were observed. This fact triggered a parallel investigation on the nature of these deposits and the vibration signatures that characterize them.

This research was developed in 3 steps:

- Micro-crystallization studies
- Interaction studies of 2,4-DNT with Ottawa Sand.
- Environmental effects on mixtures 2,4-DNT/Ottawa Sand.

5.1 Micro-Crystallization of 2,4 DNT.

Crystallization studies of 2,4-DNT in the laboratory is important because the process can be similar to that it happens when the explosive leaves the case of a mine, it is partially dissolved in water and then emerges to the soil surface forming crystals.

Figure 5.1 shows 2, 4-DNT crystals obtained by successive transfer at up to 30 times of 1 µg/µL 2,4-DNT standard solution in acetonitrile. After each deposit on gold slide a 5-minute minimum time lapse was waited to allow for solvent evaporation. Droplets are obtained with spherical and ellipsoidal form. No visible crystals were

produced immediately. Instead droplets are the only form observed. The explanation for this takes root in the fact that DNT has a melting transition at 353 K and exists like a supercooled liquid at 300 K, so DNT is observed as a metastable liquid at room temperature [Federoff, 1980]. DNT in this metastable liquid can be converted to the solid phase via a perturbation. The instability can result by further addition of solution until the density reaches a critical amount. In this way the elongated form of the globules and eventually the crystals are produced.

a.

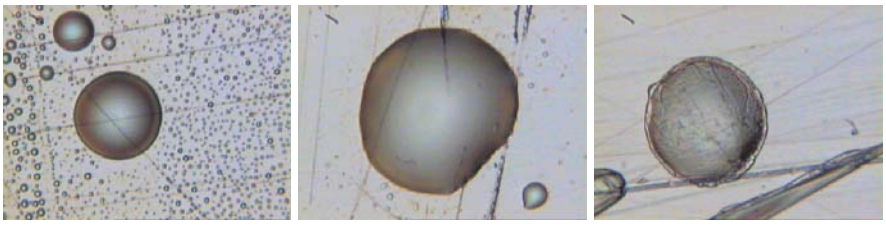

5μL 10μL 15μL

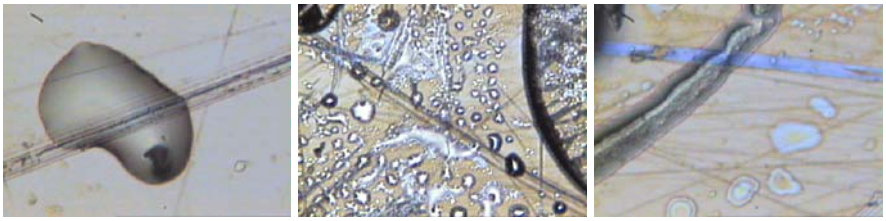

18μL 35μL 65μL

b.

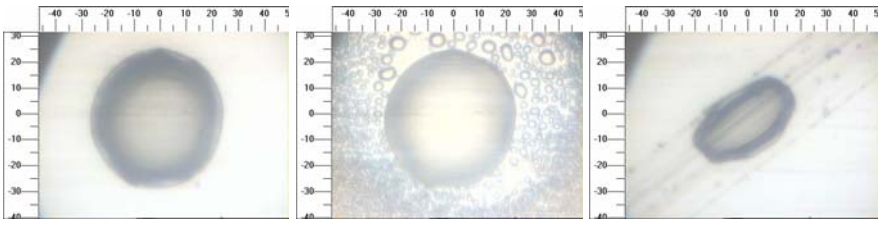

5μL 10μL 25μL

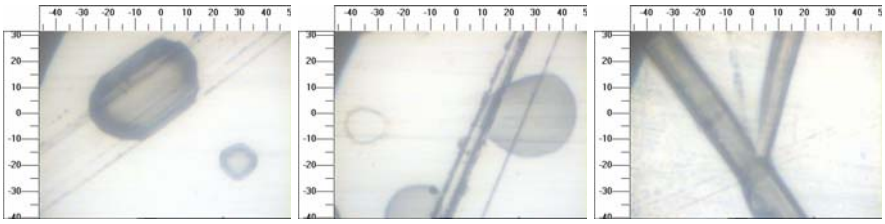

28μL 45 μL 165μL

c.

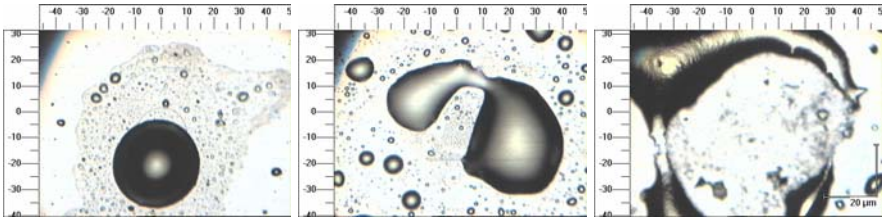

5μL 15μL 20μL

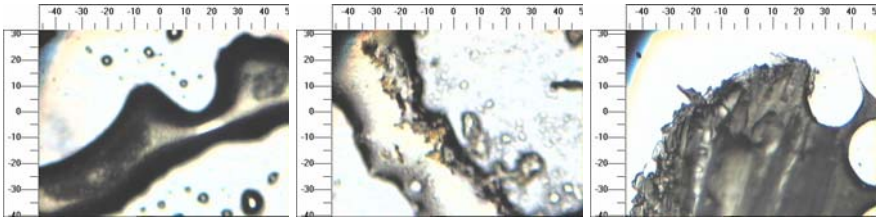

25μL 40μL 145μL

Figure 5.1 a, b, c. Formation of crystals of 2,4-DNT.

5.1.1 Raman Analysis of 2,4-DNT Droplets from Standard Solution.

Figure 5.2 shows a typical Raman Shift spectrum of the apparently amorphous DNT deposits on gold substrates. No signals from the acetonitrile solvent were found in any of the droplets analyzed. According to the literature 2,4-DNT is characterized by six prominent bands in the 750-1650 cm^{-1} region: a very strong peak at 1350 cm^{-1}, (NO_2 symmetric stretching mode), two bands at 1514 (asymmetric NO_2 stretching) and 1607 cm^{-1} (Aromatic - NO_2 conjugation), one band at 1193 cm^{-1} (C-H in plane bends), a band

at 1075 cm^{-1} (C-N-O bending mode) and one band at 792 cm^{-1} (C-H out-of-plane bend) [Clarkson et al, 2003].

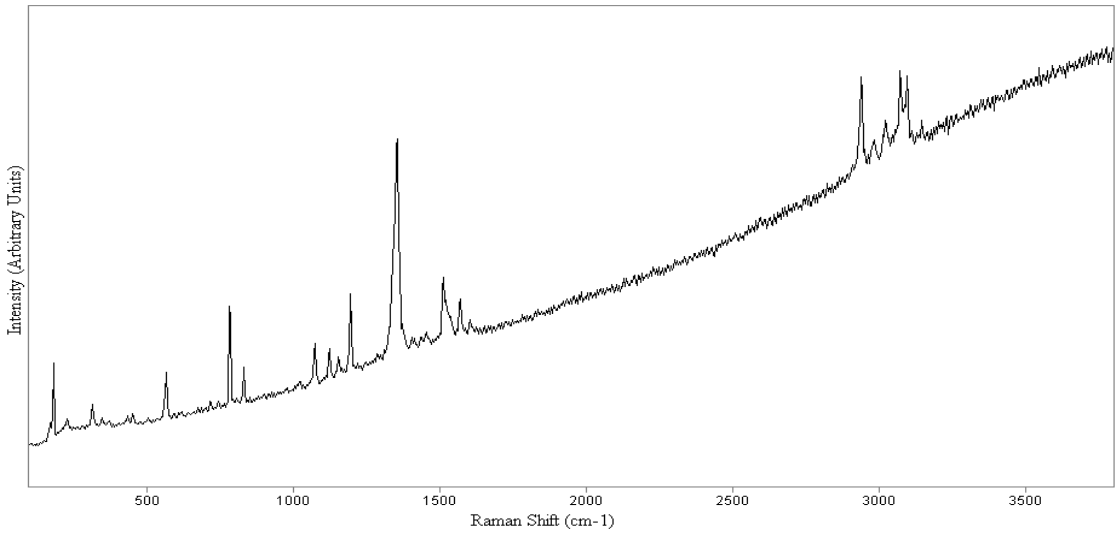

Figure 5.2 Raman spectrum of a droplet of 2,4-DNT.

Figure 5.3 shows a white light micrograph of 2,4-DNT sample obtained by transferring 10 μL of 1000 ppm standard solution of 2,4-DNT in acetonitrile. The Raman Shift spectrum was acquired using the 514.5 nm excitation source. This spectrum shows that a droplet only 10 μL has all the characteristic signals of a neat DNT sample and accounts for all the vibrational signatures reported in the literature for 2,4-DNT. The small droplet was burned by the laser action, as shown in. This is typical of these amorphous mass deposits, the total mass deposited in area is relatively large surface area and the numbers of molecules in the path of laser very small and was observed the laser damage.

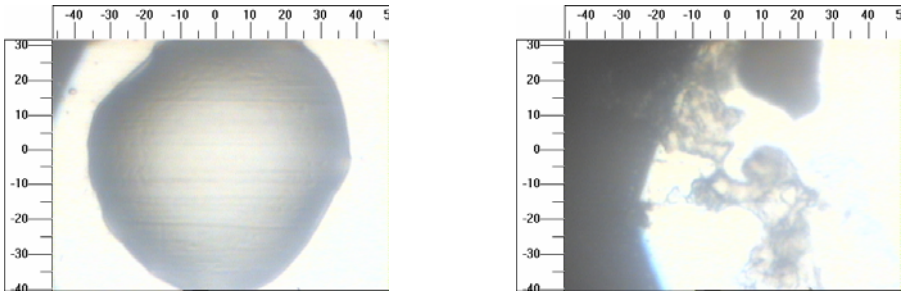

(a) **(b)**

Figure 5.3 White Light Micrograph of a 2,4-DNT droplet. (a) before and (b) after taking the Raman Spectrum.

5.1.2 Region from 200 cm^{-1} to 1000 cm^{-1}

Figure 5.2 shows the full Raman Shift spectrum for a DNT droplet. It is of interest to discuss the Raman signatures in three regions: 200 -1000 cm^{-1}, 1000 -1800 cm^{-1}, 2700 - 3600 cm^{-1}. The most important Raman signature in this region is the band at 780 cm^{-1} in which assigned to Nitro group scissoring mode. A band at 830 cm^{-1} is assigned to methyl rock vibration. No prominent bands are present in the 100-500 cm^{-1} region.

5.1.3 Region from 1000 cm^{-1} to 1800 cm^{-1}

This spectral region is equivalent to the infrared fingerprint region, where all strong group vibrations occur. It is of interest to discuss the Raman signatures in three regions: 200 -1000 cm^{-1}, 1000 -1800 cm^{-1}, 2700 - 3600 cm^{-1}. The strongest Raman signals are found in this region. The vibration mode assigned to the C-N-O bending appears at 1075 cm^{-1} the band at 1123 cm^{-1} is assigned to methyl H-C-H asymmetric bend. The band found at 1193 cm^{-1} was assigned to the H-C-C in plane bending

movement. The very strong band at 1350 cm^{-1} was assigned to the symmetric NO_2 stretching vibration. The band to 1607 cm^{-1} was assigned to aromatic - NO2 conjugation.

5.1.4 Region from 2700 cm^{-1} to 3600 cm^{-1}

This region shows four prominent signals. The Raman Shift signal at 2940 cm^{-1} was assigned to asymmetric C-H vibration of the CH3 group. The band found to 3021 cm^{-1} was assigned to mode aromatic C-H stretch vibration. The peak found in the droplets at 3100 cm^{-1} corresponds to aromatic C-H stretch vibration. This asymmetric stretching C-H mode is split into a doublet at 3070 cm^{-1} and 3100 cm^{-1}.

5.1.5 Raman Analysis of 2,4-DNT Crystals from standard solution.

2,4-DNT crystals were obtained by successive pipette transfer of up to 30 times of solution of nominal concentration of 5 µg/µL 2,4-DNT standard solution. After each transfer a 5 minute minimum time lapse was waited to allow for solvent evaporation. Figure 5.4 illustrates the white light micrographs of the crystals.

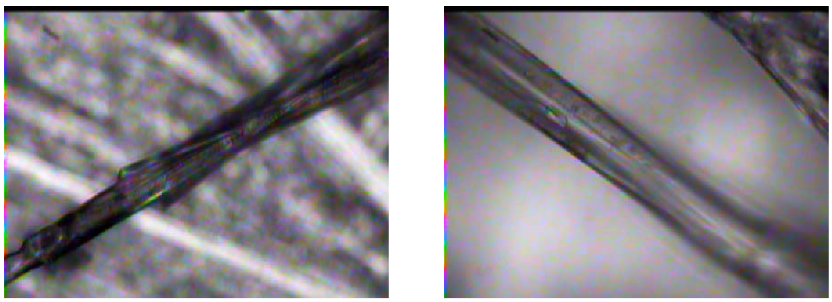

130 µL 160 µL

Figure 5.4 Micrographs of Crystals of 2,4-DNT crystals obtained by pipette transferring and evaporation of acetonitrile.

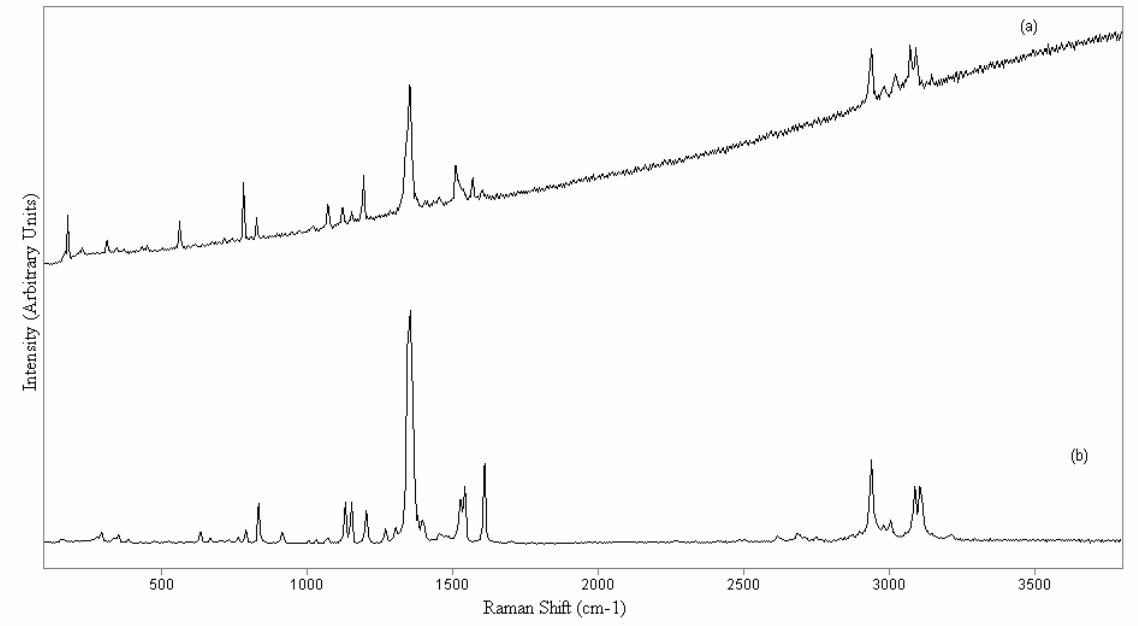

Figure 5.5 Comparison of spectra of 2,4-DNT:
(a) droplet, (b) crystal

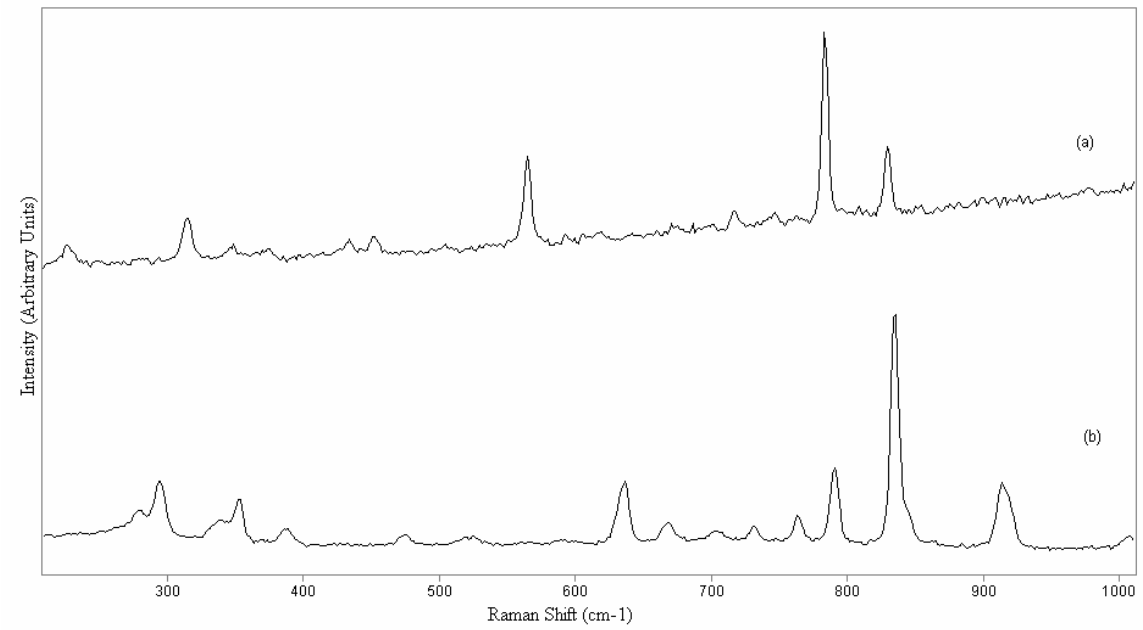

Figure 5.6 Comparison of spectra of 2,4-DNT region 200 – 1000 cm^{-1}:
(a) droplet, (b) crystal

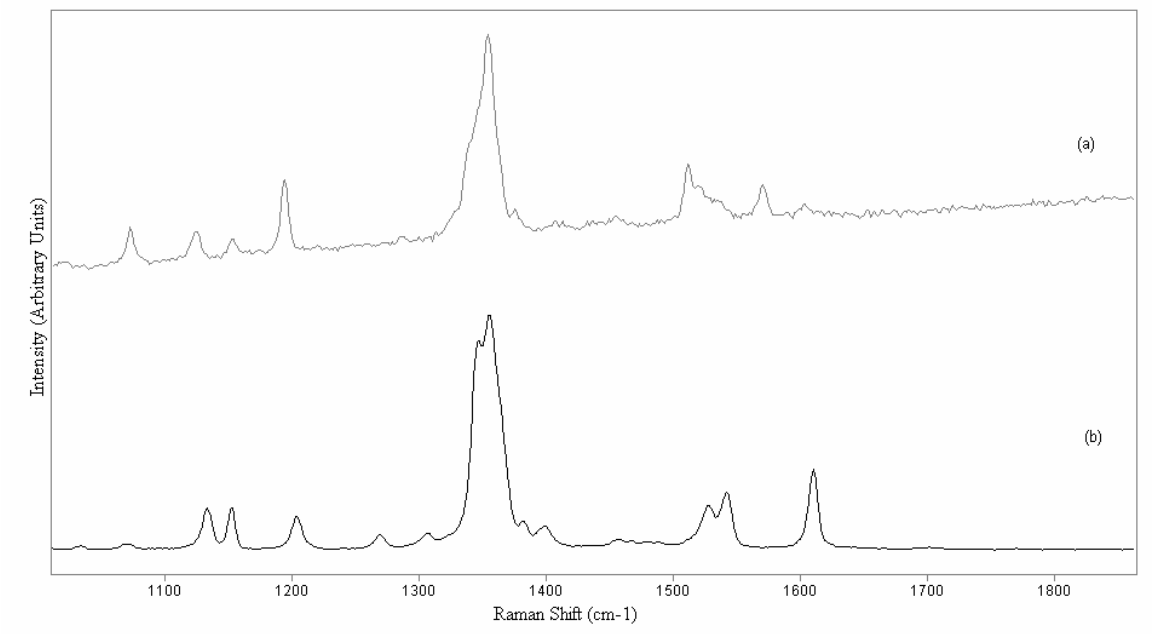

Figure 5.7 Comparison of spectra of 2,4-DNT region 1000 – 1800 cm^{-1}:
(a) droplet, (b) crystal

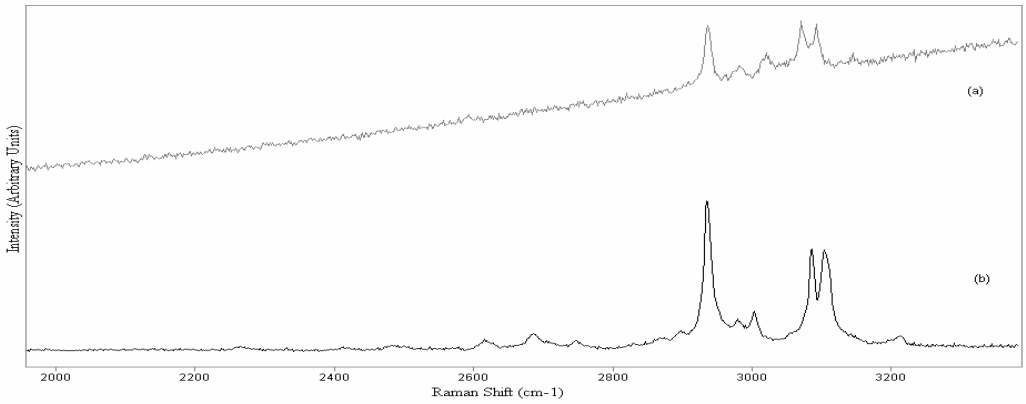

Figure 5.8 Comparison of spectra of 2,4-DNT region 2000 – 3400 cm^{-1}:
(a) droplet, (b) crystal

After depositing aliquots of 5.µL of 5 µg/µL 2,4-DNT standard solution the droplets continued to grow by mass accumulation due to the evaporation of solvent. As the number of transfers increase, the droplet size is increased, an eventually crystals form.

Figure 5.4 shows that after depositing 130 µL of DNT standard solution, 2,4-DNT crystals are produced at ambient temperature.

Typical Raman Shift spectrum using 514 nm excitation line in the 100-3800 cm^{-1} region of crystals of 2,4-DNT obtained from crystal formation by standard solution is shown in Figure 5.5 (b). Raman signatures (peaks) that allow identifying the 2,4-DNT are those corresponding to a 1350 cm^{-1} (NO_2 symmetric stretching vibration) and 830 cm^{-1} (methyl rock). Here, also, it is interesting to note that some characteristic bands of 2,4-DNT such as 1514 cm^{-1} (asymmetric NO_2 stretching), 1607 cm^{-1} (aromatic NO_2 conjugation), 1193 cm^{-1} (C-H in plane bend), and 780 cm^{-1} (nitro-group scissoring mode). Similarly, as in the spectrum of DNT droplets it can be observed that in the 100-500 cm^{-1} region no prominent bands are present.

The Raman Shift spectrum of 2,4-DNT crystals is similar to the Raman spectra of the droplets in the Figure 5.5 however, as can be noted there are signals that do not correspond in one or the other spectra. It is also important to note that the relative intensities of the lesser intense bands do not correspond. This indicates that the crystal form and the suspected amorphous form are not equivalent.

In the 200 to 1000 cm^{-1} region the signals about 634 cm^{-1}, 668 cm^{-1}, 912 cm^{-1} did not appear in the spectrum of the droplet (Fig. 5.6). From 1000-1800 cm^{-1} (Fig. 5.7) the signals at 1269 cm^{-1} and 1398 cm^{-1} appear in spectrum of crystal are not present in spectrum of the DNT droplet. In the 2000-3600 cm^{-1} region (Fig. 5.8) shows bands with higher intensity and better definition about 3000 cm^{-1}. Very weak intensity signals corresponding to the C-H stretch vibrations of aliphatic CH_3 group. At 1263 and 1301 cm^{-1}, there are two bands that did not appear in the spectrum of droplet of 2,4-DNT.

Table 5.1 Raman Shift Assignments for 2,4-DNT.

Raman cm^{-1}	**Tentative Assignment 2,4-DNT**
3100 (w)	aromatic C-H stretch vibration
3070 (w)	aromatic C-H stretch vibration
3021 (w)	aromatic C-H stretch vibration
2940 (s)	asymmetric C-H vibration of the CH_3 group
1607 (s)	aromatic- NO_2 conjugation
1514 (s)	asymmetric NO_2 stretching vibration
1445 (w)	C-C ring stretch
1350 (s)	symmetric NO_2 stretching vibration
1193 (m)	H-C-C in plane bend
1147 (vw)	symmetric methyl H-C –H bend
1123 (w)	methyl H-C-H asymmetric bend
1075 (vw)	C-N-Ó bend
1020 (w)	Out- of- plane bend of ring H
830 (w)	methyl rock
792(w)	out-of- plane C-H and C-N bend
780 (m))	Nitro-group scissoring mode
717 (vw)	C-N-Ó bend
560 (vw)	ring deformation
100-500	Skeletal deformation of the aromatic ring

vs = very strong; s = strong; m = medium; w = weak; vw = very weak.

5.2 Interaction of 2,4-DNT with Ottawa Sand

The following step was to prepare mixtures of Ottawa sand with 2,4-DNT. Samples with several Ottawa sand / 2,4 DNT proportions (Table 5.2) were prepared and mixed with a digital mixer (Vortex™) during 5 minutes at 3000 rpm. Their Raman Shift spectra were then collected and compared with that of neat 2,4-DNT crystals.

Table 5.2 Preparation of different mixtures of sand /explosive

Proportion	Ottawa Sand (g)	2,4-DNT (g)
1:1	0.1	0.1
10:1	1	0.1
100:1	1	0.01
1000:1	1	0.001
10000:1	1	0.0001

5.2.1 Mixture of 1:1 Ottawa Sand/2,4-DNT.

Figure 5.9 shows the spectra of: (a) the neat crystals supplied by Chem Service Inc, (b) of a 1:1 mixture of 0.1 g Ottawa Sand plus 0.1 g 2,4-DNT. Displacement in the Raman bands was observed for the mixture with a 1:1 ratio. The bands are listed in Table 5.3. The peak at 1020 cm^{-1} assigned to out of plane bend of ring H showed a shift of 3 cm^{-1} in Figure 5.10. For the band assigned to methyl H-C-H asymmetric bend appearing 1123 cm^{-1} a shift of 2 was observed (see Figure 5.11). The displacement of the band assigned to asymmetric NO_2 was 4 cm^{-1}, the signal at 1514 cm^{-1} that is assigned to asymmetric NO_2 stretching vibration showed a shift of 9 cm^{-1}. In Figure 5.12 the band at 2940 cm^{-1} showed a shift of 4 cm^{-1}.

Table 5.3 Raman Displacement of the Ottawa sand /2,4–DNT Mixtures

Raman (cm^{-1})	**Tentative Assignment of bands 2,4 DNT**	**1:1**	**10:1**	**100:1**	**1000:1**	**10000:1**
3100	aromatic C-H strech vibration	0	-10	26	-31	-41
2940	asymmetric C-H vibration	4	4	16	-26	-26
1607(s)	aromatic- NO_2 conjugation	0	-6	-21	-26	-30
1514(s)	asymmetric NO_2 stretching vibration	-9	-9	-17	-22	-31
1350(vs)	symmetric NO_2 stretching vibration	-4	-6	-22	-25	-29
1193(m)	H-C-C in plane bend	0	-2	-6	-26	-29
1147(vw)	symmetric methyl H-C-H bend	0	- 2	-14	-17	-23
1123(w)	methyl H-C-H asymmetric bend	-2	-3	-13	-25	-31
1020(w)	out – of – plane bend of ring H	0	-2	-17	-15	-25
830(m)	Metyl rock mode	0	-4	-20	-26	-37
717(w)	C- H – of – plane and C-N bend	0	0	-16	-21	-29

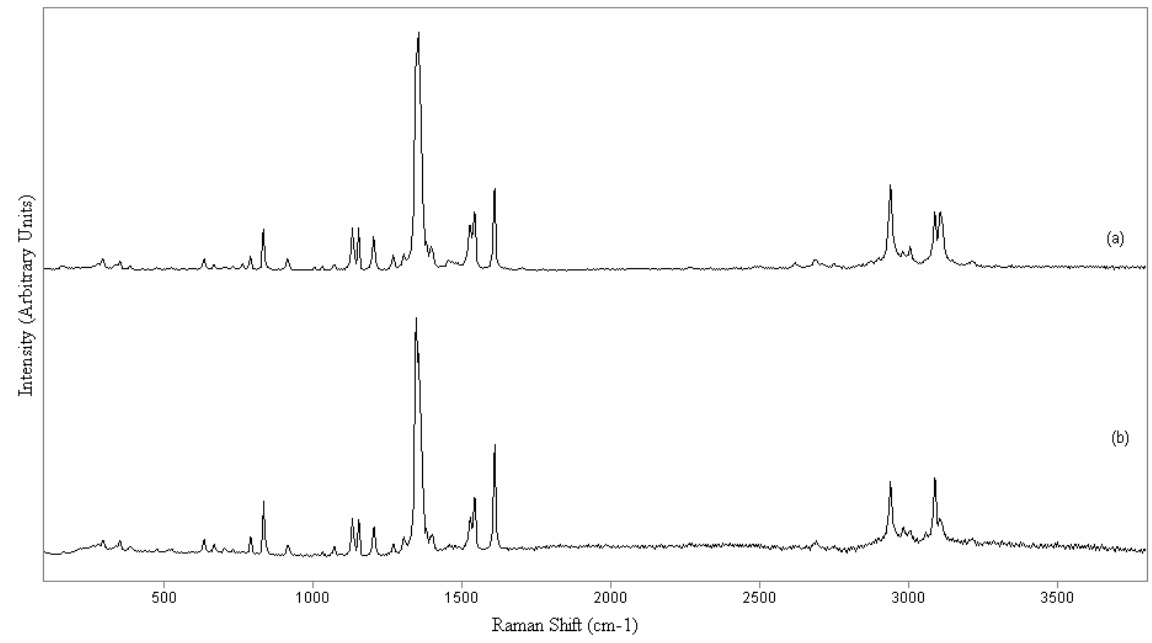

Figure 5.9 Full Raman spectra (a) neat 2,4-DNT crystals, (b) Mix 1:1 Ottawa Sand/2,4-DNT.

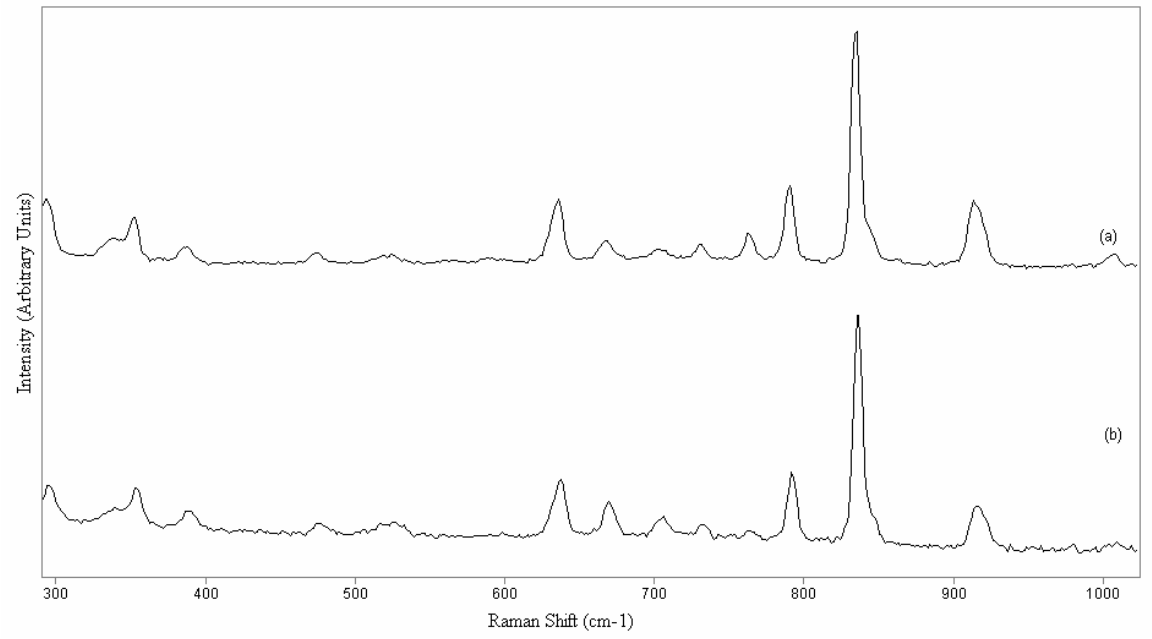

Figure 5.10 Raman shift region of 200-1000 cm^{-1}(a) pure 2,4-DNT, (b) Mix 1:1 Ottawa Sand/2,4-DNT.

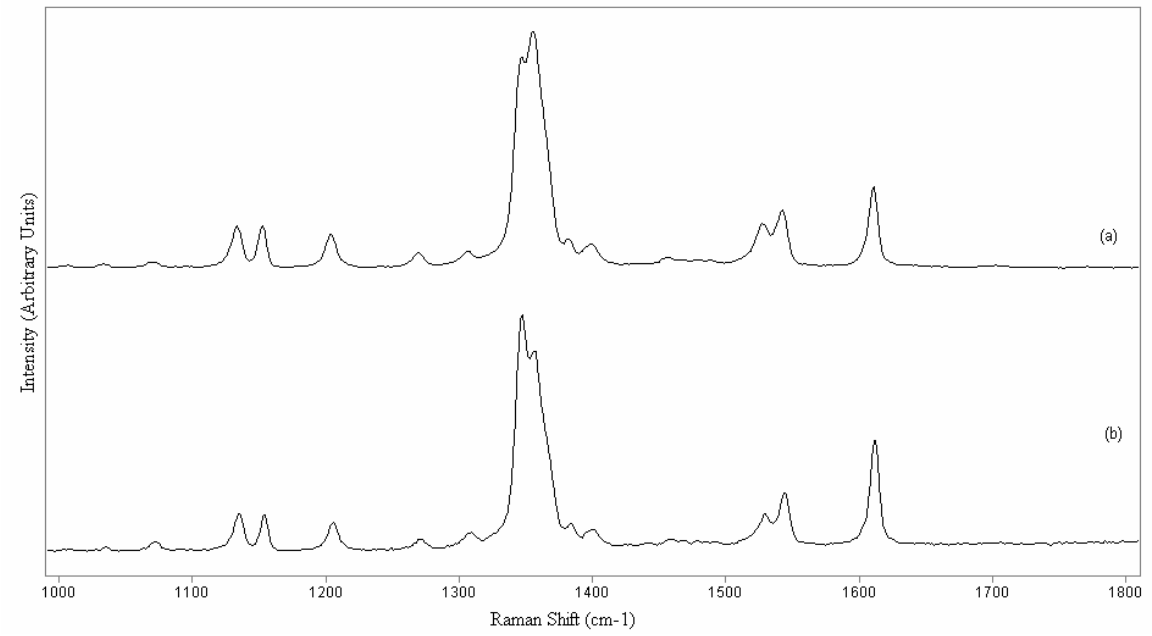

Figure 5.11 Raman shift region 1000-1800 cm^{-1}: (a) pure 2,4-DNT, (b) Mix 1:1 Ottawa Sand/2,4-DNT.

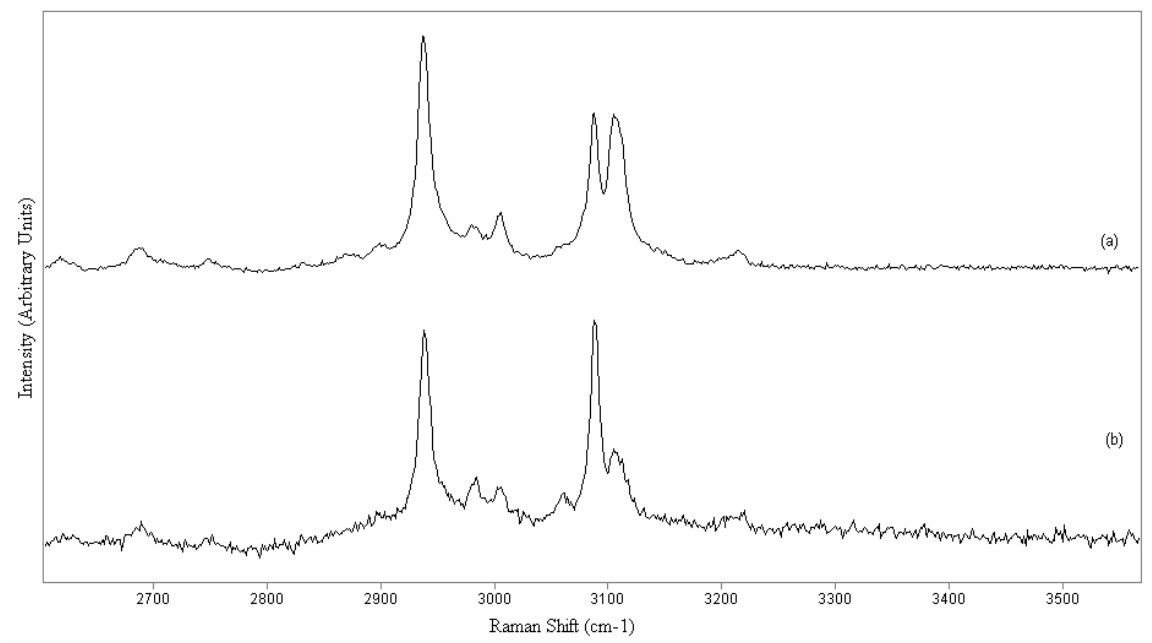

Figure 5.12 Raman shift region 2700 -3600 cm^{-1}(a) pure 2,4-DNT, (b) Mix 1:1 Ottawa Sand/2,4-DNT.

5.2.2 Mixture of 10:1 Ottawa Sand/2,4-DNT.

Figures 5.13 to 5.16 show the Raman Shift spectra at different regions, that were obtained of mixture of 1 g of Ottawa sand and 0.1g of 2,4-DNT. In Figure 5.14 the band at 830 cm^{-1} that is assigned to methyl rock mode shows a shift of – 4 cm^{-1}. The band assigned to out-of-plane bend of ring H at 1020 cm^{-1} shows a shift of – 3 cm^{-1} and the signal at1123 cm^{-1} that was assigned methyl H-C-H asymmetric bend showed a shift of – 2 cm^{-1} (see Figures 5.14 – 5.16). At 1193 cm^{-1} for the signal that was assigned to H-C-C in plane bend showed a shift of – 3 cm^{-1}. The Raman signature at 1350 cm^{-1} for the symmetric NO_2 stretching vibration shows a change at – 6 cm^{-1}, to 1514 cm^{-1} the band assigned to asymmetric NO_2 stretching vibration that showed at of –9 cm^{-1} and of the

band to 1607 cm^{-1} assigned to aromatic- NO_2 conjugation was displaced by – 6 cm^{-1}. The band assigned to aromatic C-H stretch vibration at 3100 cm^{-1} showed shits of – 10 cm^{-1}.

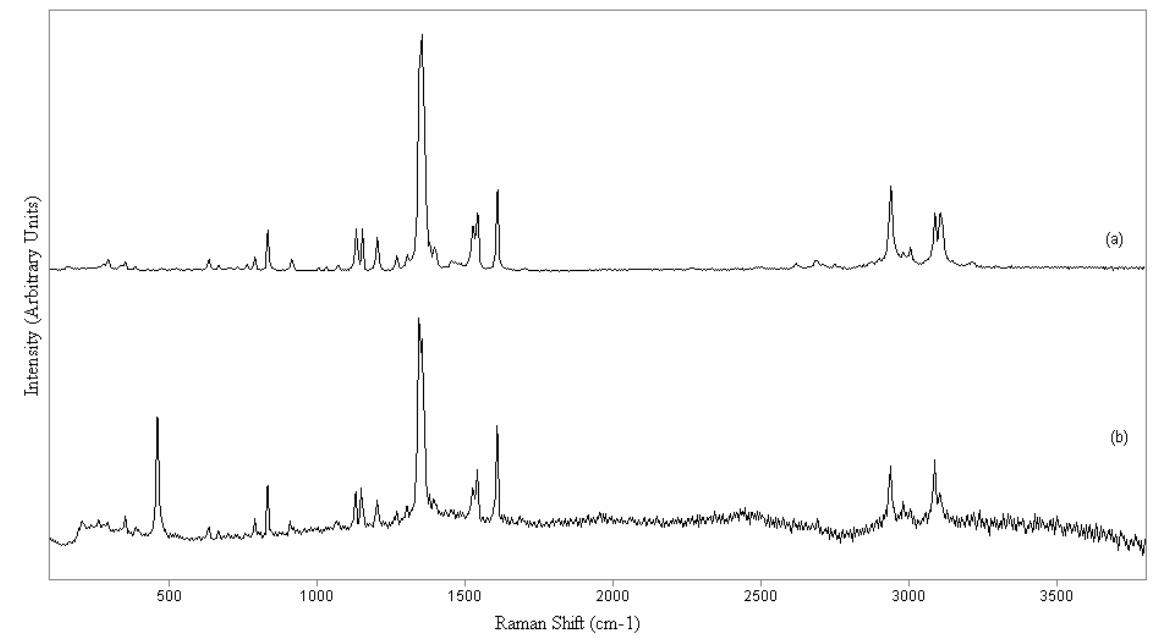

Figure 5.13 (a) pure 2,4-DNT, (b) Mix 10:1 Ottawa Sand/2,4-DNT.

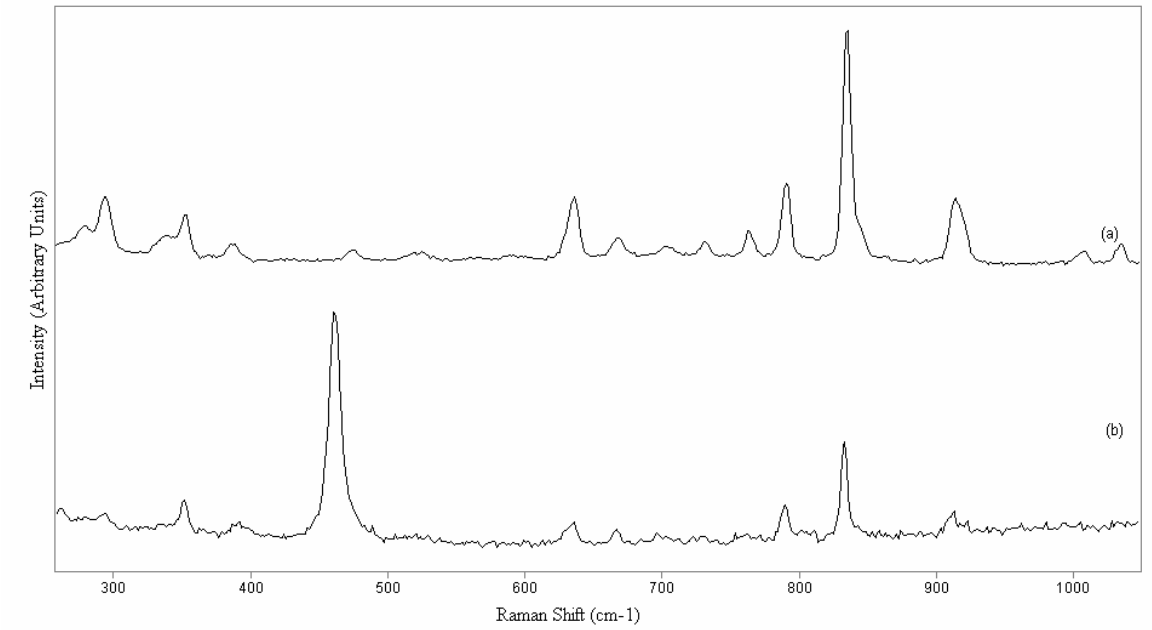

Figure 5.14 Raman shift region 200-1000 cm^{-1} of: (a) pure 2,4-DNT, (b) Mix 10:1 Ottawa Sand/2,4-DNT.

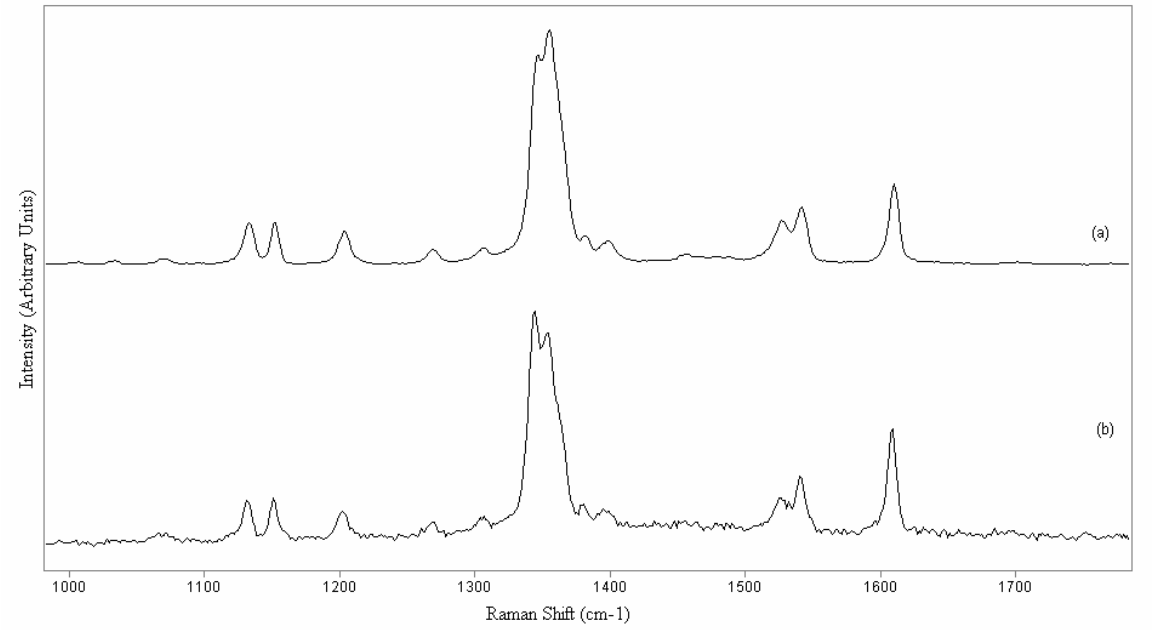

Figure 5.15 Raman shift region 1000-1800 cm $^{-1}$ (a) pure 2,4-DNT, (b) Mix 10:1 Ottawa Sand/2,4-DNT.

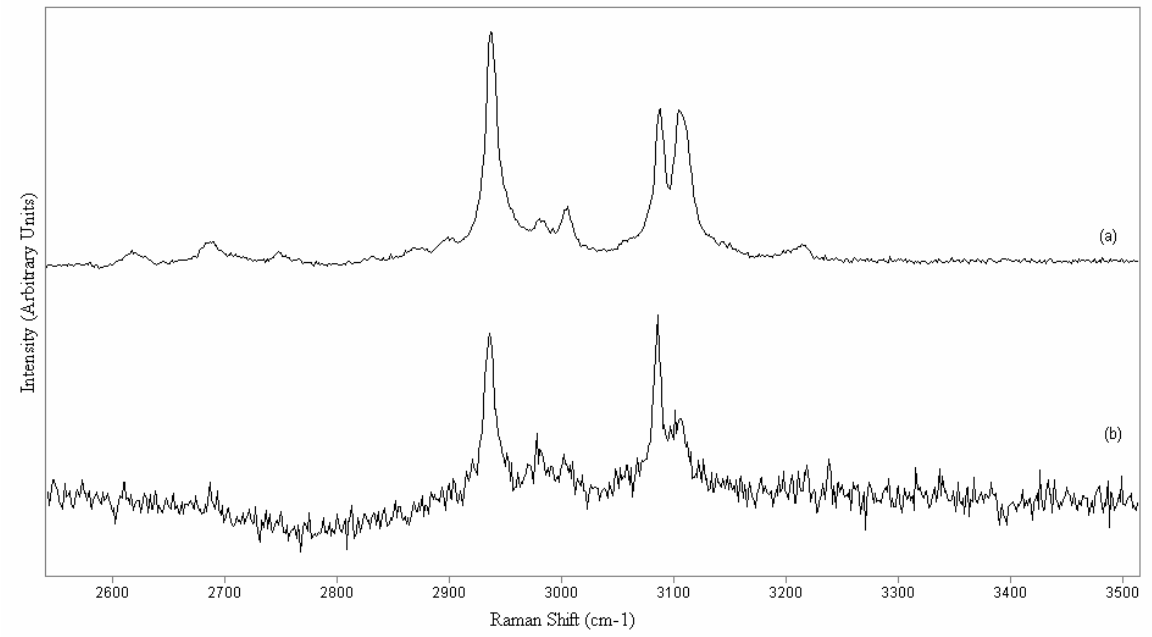

Figure 5.16 Raman shift region 2700-3600 cm $^{-1}$ (a) pure 2,4-DNT, (b) Mix 10:1 Ottawa Sand/2,4-DNT.

5.2.3 Mixture of 100:1 Ottawa Sand/2,4-DNT.

Figure 5.17 shows the Raman Spectra of mixture of Ottawa sand and 2,4-DNT in a 100:1 proportion obtained by mixing 1 g of Ottawa sand and 0.001 g of 2,4-DNT. In Figure 5.18-5.20 the band at 717 cm^{-1}, assigned to C-N-O bend, showed a shift of – 16 cm^{-1}. The signal assigned to nitro group scissoring mode at 830 cm^{-1} showed a shift of – 20 cm^{-1}. The band assigned to out-of-plane bend of ring H at 1020 cm^{-1} shifted by -13 cm^{-1}. The band to 1147 cm^{-1} assigned to symmetric H-C-H in plane bend showed a shift of – 14 cm^{-1}, the band to 1193 cm^{-1} that was assigned to Symmetric methyl H-C-H bend showed a shift of -6 cm^{-1}, a shift of – 22 cm^{-1} of the band assigned to symmetric NO_2 at 1350 cm^{-1} was observed. In range of 2700-3600 cm^{-1} the band at 2940 cm^{-1} assigned to asymmetric C-H vibration showed a shift of 16 cm^{-1} . The band at 3100 cm^{-1} of aromatic C-H stretch vibration shifted by – 26 cm^{-1}.

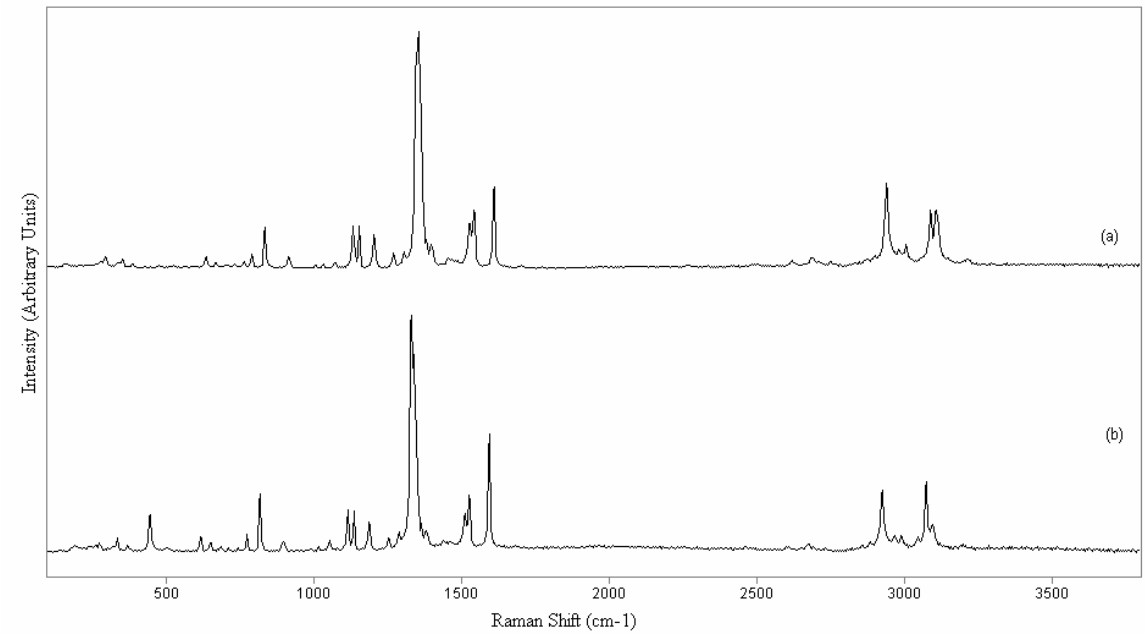

Figure 5.17 : (a) pure 2,4-DNT, (b) Mix 100:1 Ottawa Sand/2,4-DNT.

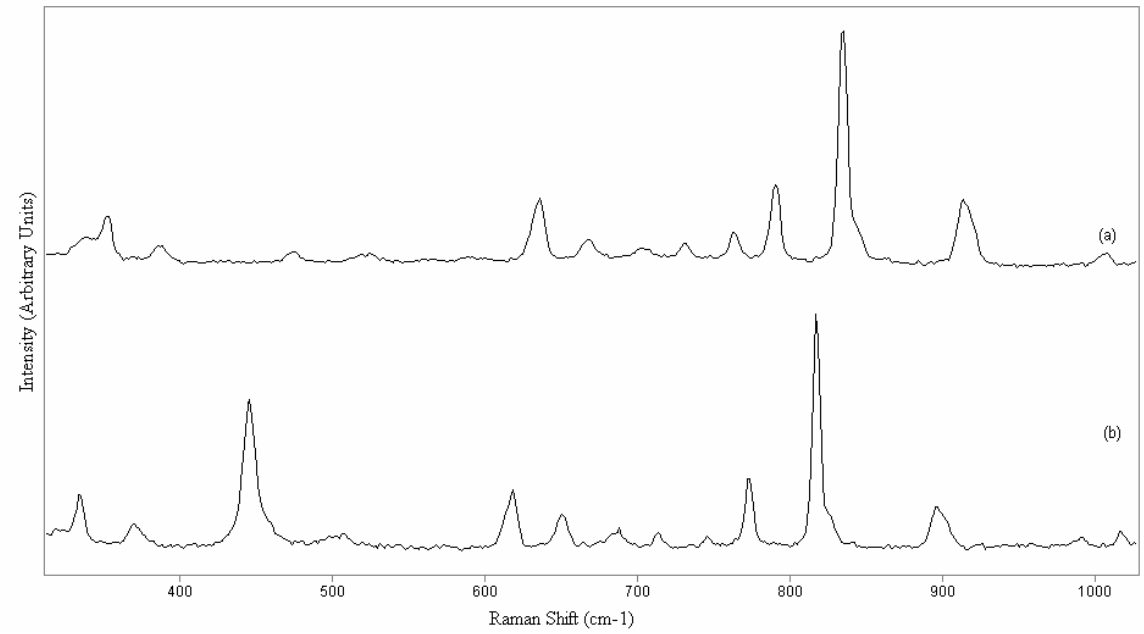

Figure 5.18 Raman shift region 200-1000 cm $^{-1}$ (a) neat 2,4-DNT crystals, (b) Mix 100:1 Ottawa Sand/2,4-DNT.

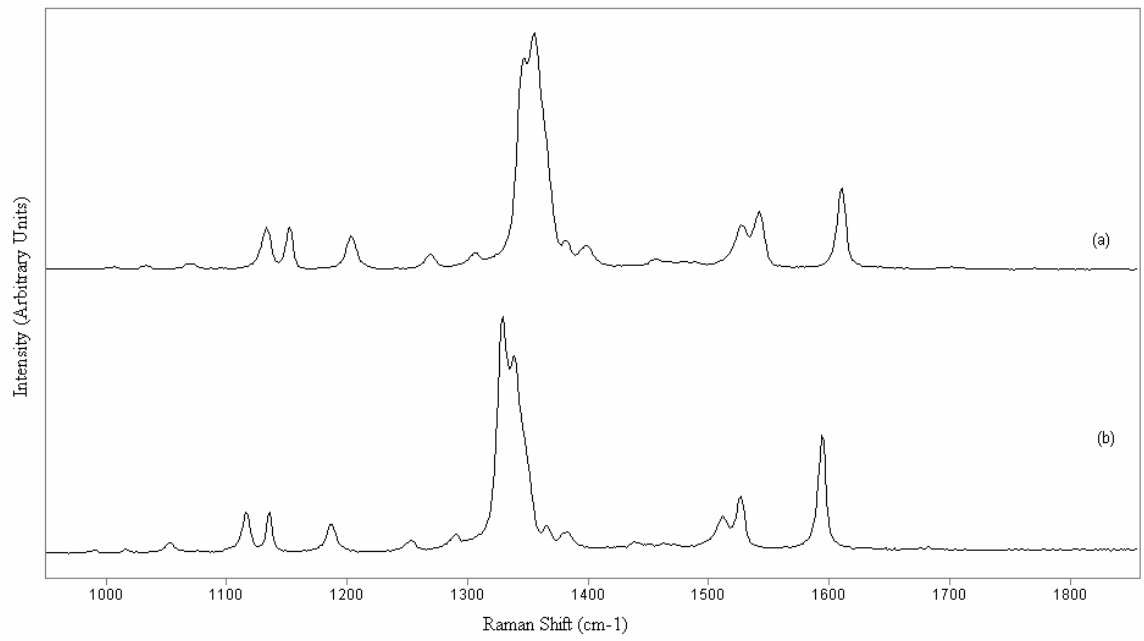

Figure 5.19 Raman shift region 1000-1800 cm $^{-1}$ (a) neat 2,4-DNT crystals , (b) Mix 100:1 Ottawa Sand/2,4-DNT.

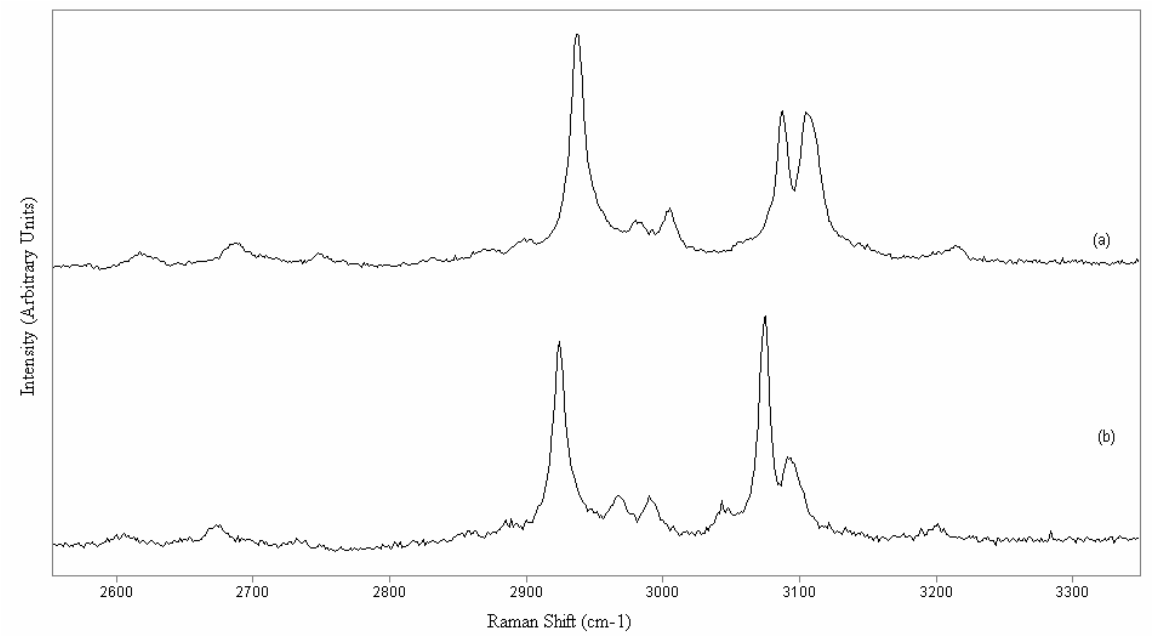

Figure 5.20 Raman shift region 2600-3600 cm $^{-1}$ (a) neat 2,4-DNT crystals , (b) Mix 100:1 Ottawa Sand/2,4-DNT.

5.2.4 Mixture of 1000:1 Ottawa Sand/2,4-DNT.

The Raman spectrum of the 1000:1 mixture is shown in Figures 5.21-5.24. The band of 792 cm^{-1} assigned to C – H – of – plane band and C-N bend showed a shift of – 21 cm^{-1}. The band of 830 cm^{-1} assigned to methyl rock mode has a shift of – 26 cm^{-1}. The band of 1020 cm^{-1} that was assigned to out of plane bend showed a shift of 15 cm^{-1}, the band of 1123 cm^{-1} has a shift of 25 cm^{-1} , the band of 1147 cm^{-1} assigned to symmetric Methyl H-C-H bend shows a shift of –17cm^{-1}. The band at 1193 cm^{-1} assigned to H-C-C in plane bend showed a shift of –26 cm^{-1}.

In Figure 5.23 the band at 1350 cm^{-1} assigned to symmetric NO_2 stretching vibration shows a shift of – 25cm^{-1}, the band of 1514 cm^{-1} has a shift of – 22 cm^{-1} and the band assigned to aromatic- NO_2 conjugation showed a shift of – 26cm^{-1}, at 1607 cm^{-1}. In

Figure 5.23 the band at 2940 cm^{-1} showed a shift of - 26 cm^{-1} and the band at 3100 cm^{-1} has a shift of - 31 cm^{-1}.

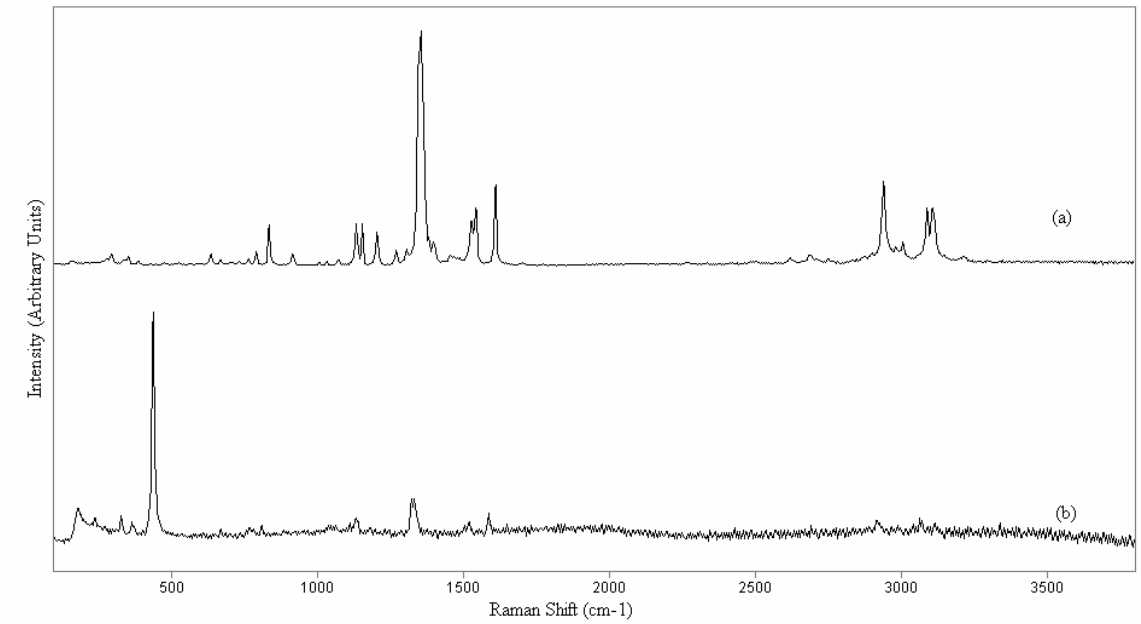

Figure 5.21 Full Raman spectra (a) neat 2,4-DNT crystals , (b) Mix 1000:1 Ottawa Sand/2,4-DNT.

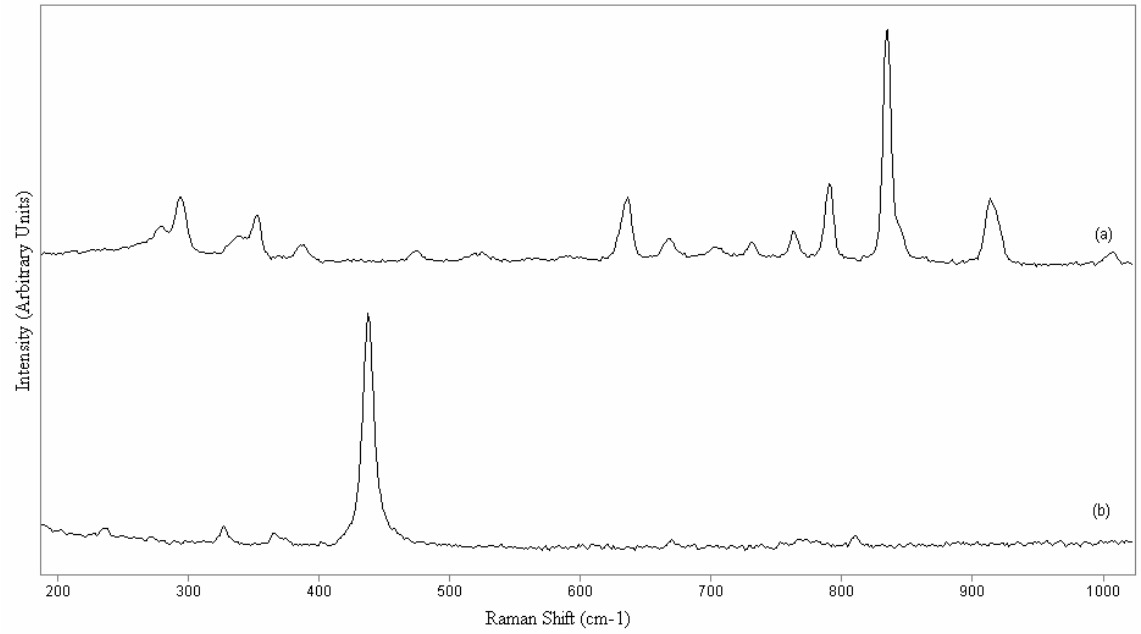

Figure 5.22 Raman spectra region 200-1000 cm^{-1} (a) neat 2,4-DNT crystals , (b) Mix 1000:1 Ottawa Sand/2,4-DNT.

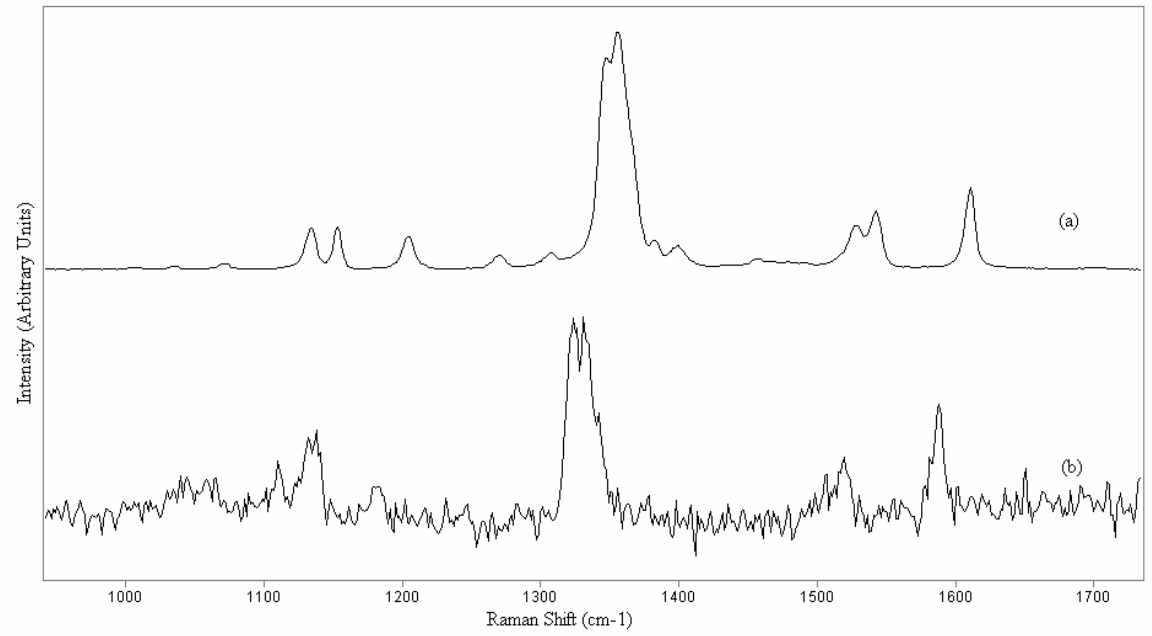

Figure 5.23 Raman spectra region 1000- 1800 cm $^{-1}$ (a) neat 2,4-DNT crystals , (b) Mix 1000:1 Ottawa Sand/2,4-DNT.

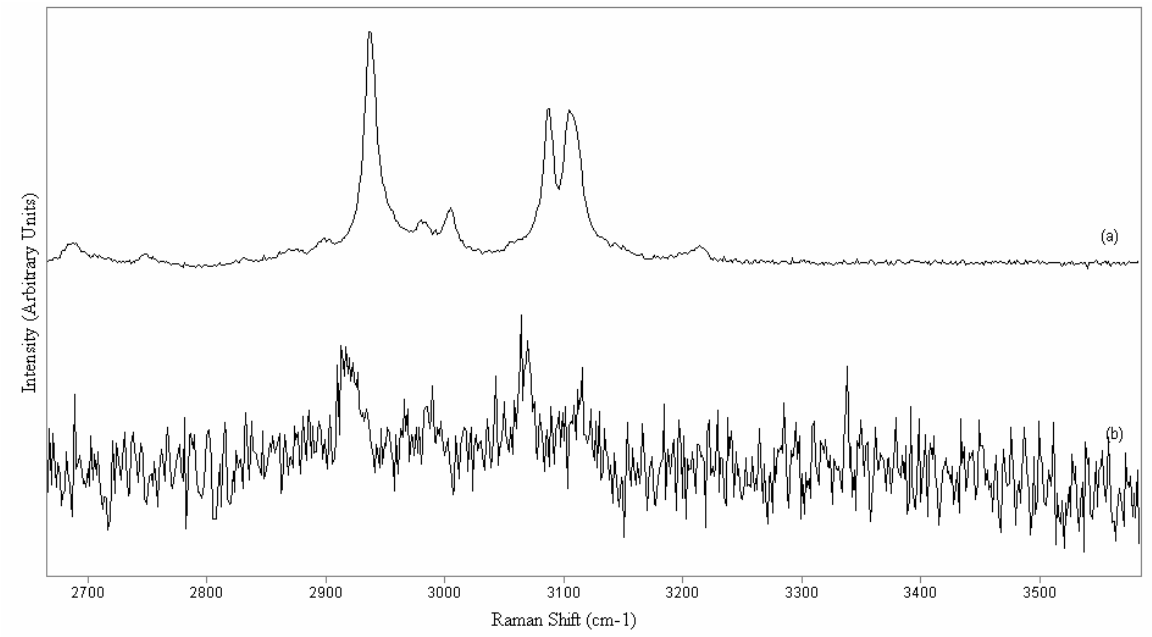

Figure 5.24 Raman spectra region 2600- 3600 cm $^{-1}$ (a) neat 2,4-DNT crystals , (b) Mix 1000:1 Ottawa Sand/2,4-DNT.

5.2.5 Mixture of 10000:1 Ottawa Sand/2,4-DNT.

Figure 5.25 shows the Raman spectrum of 2,4 DNT of the mixture of 10000:1 of Ottawa Sand and 2,4-DNT. The largest shift in the Raman bands was observed for the mixture with a 10000:1 ratio and the bands that indicated a stronger interaction was 1350 cm^{-1} symmetric NO_2 stretching vibration. This could point to a DNT – sand interaction via nitro groups of DNT.

In Figure 5.27 the Raman spectrum can be observed the band at 1350 cm^{-1} assigned to symmetric NO_2 stretching vibration a shift to –29cm^{-1}, the band of 1514cm^{-1} have a shift of –22 cm^{-1} and the band assigned to aromatic- NO_2 conjugation showed a shift of –26 cm^{-1} at 1607 cm^{-1}. In Figure 5.25 we can see the band of 792 cm^{-1} assigned to out of plane C-H and C-N bend showed a shift of –29 cm^{-1}, the band of 830 cm^{-1} assigned to methyl rock mode have a shift of –37 cm^{-1}, the band of 1123 cm^{-1} have a shift of 31 cm^{-1}, the band of 1147 cm^{-1} assigned to symmetric methyl H-C-H bend have a shift of –23cm^{-1}, and the band to 1193 cm^{-1} assigned to H-C-C in plane bend showed a shift of –29 cm^{-1}. The band at 2940 cm -1 showed shift of - 26 cm^{-1} and the band at 3100 cm^{-1} showed a shift of -41 cm^{-1} a strong band at 463 cm^{-1} that was assigned to Si-O of Ottawa Sand.

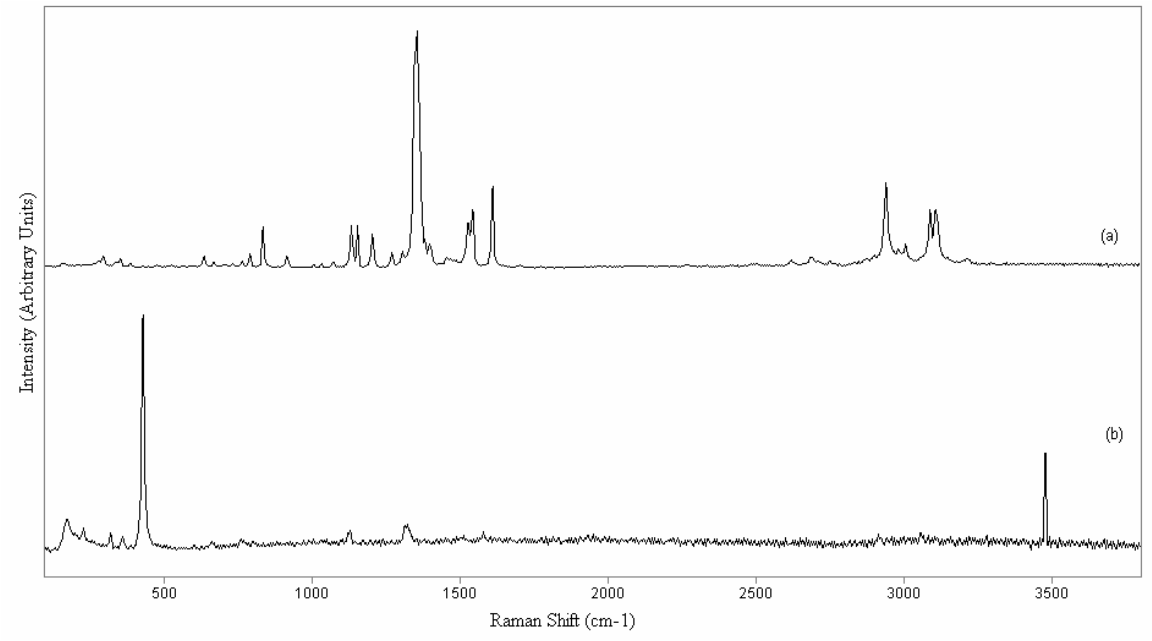

Figure 5.25 Full Raman spectra of :(a) neat 2,4-DNT crystals , (b) Mix 10000:1 Ottawa Sand/2,4-DNT.

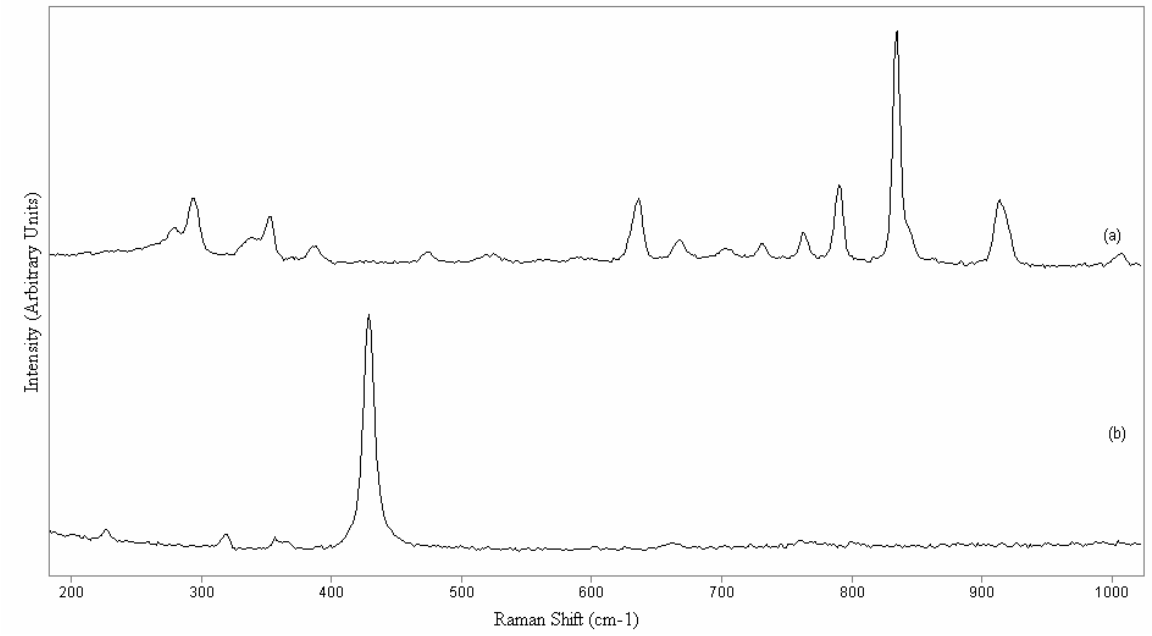

Figure 5.26 Raman spectra region 200-1000 cm $^{-1}$ (a) neat 2,4-DNT crystals , (b) Mix 10000:1 Ottawa Sand/2,4-DNT.

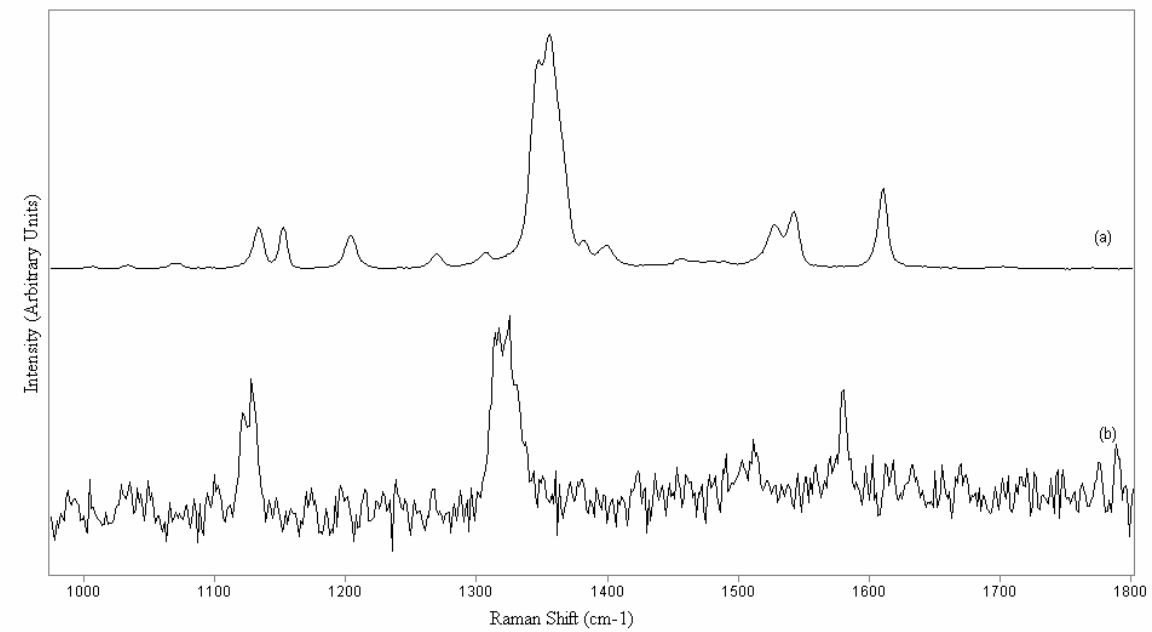

Figure 5.27 Raman spectra region 1000-1800 cm $^{-1}$ (a) neat 2,4-DNT crystals , (b) Mix 10000:1 Ottawa Sand/2,4-DNT.

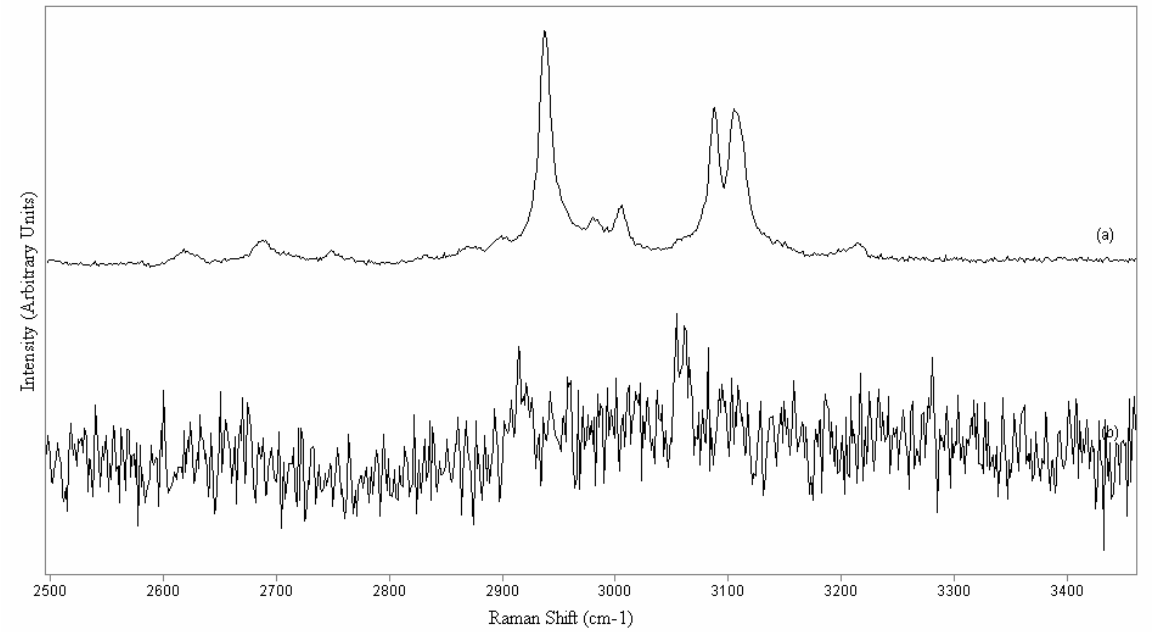

Figure 5.28 Raman spectra region 2500-3600 cm^{-1} (a) neat 2,4-DNT crystals , (b) Mix 10000:1 Ottawa Sand/2,4-DNT.

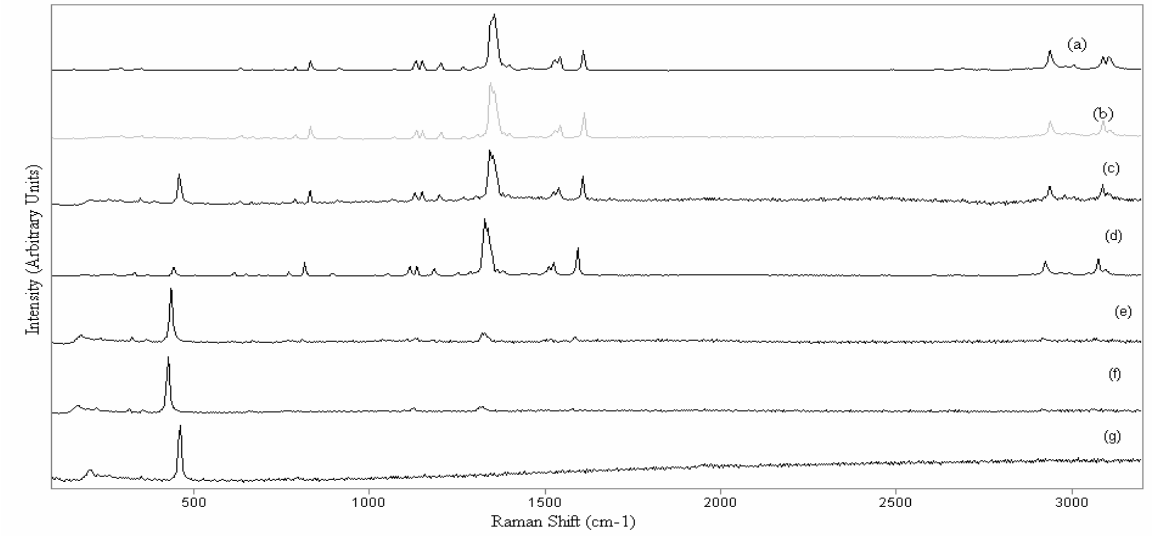

Figure 5.29 Full Raman spectra (a)2,4-DNT, (b)1/1, (c) 10/1, (d) 100/1, (e) 1000/1, (f) 10000/1, (g) Sand

Figure 5.29 shows how the characteristic vibrational signatures of 2,4-DNT appear as a function of the sand/DNT mass ratio. The signal at 490 cm^{-1} assigned to symmetric vibration –Si-O-Si (Ottawa Sand) gives a strong Raman band which also shows higher intensity as the sand component in the mixture becomes larger.

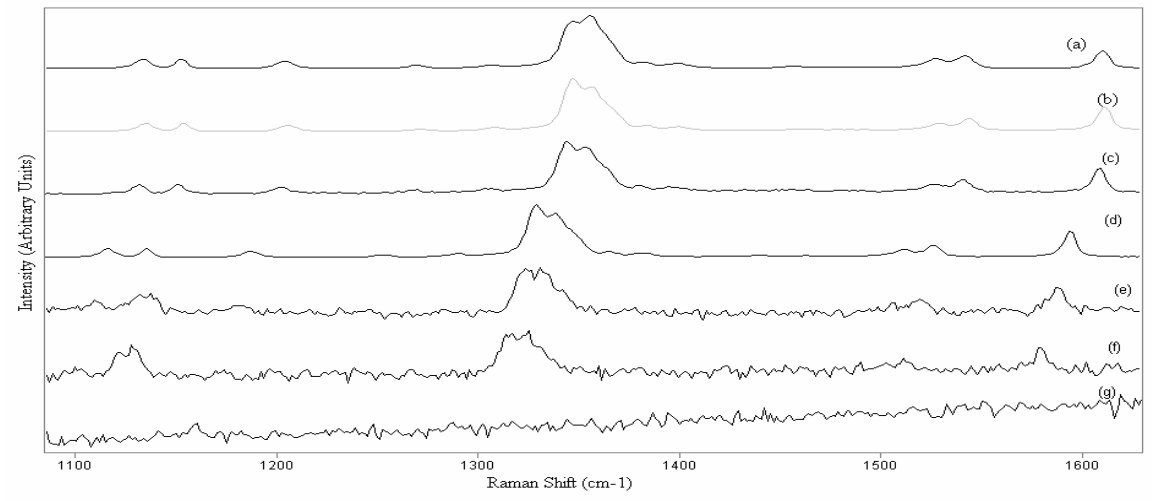

Figure 5.30 Raman spectra region 1100-1600 cm^{-1} for: (a)2,4-DNT, (b)1/1, (c) 10/1, (d) 100/1, (e) 1000/1, (f) 10000/1, (g) Sand

White light micrographs of Figure 5.31 show sand particles surrounding a small DNT crystal. Raman spectra of these particles exhibit relatively large displacements of te characteristic DNT signatures. The band shifts that are observed are contained in Table 4. In Figure 5.32 and 5.33 illustrate see the tendency of the band 1350 cm^{-1} symmetric NO_2 stretching vibration towards low wavenumbers.

Figure 5.31 Interaction of 2,4-DNT and Ottawa Sand.

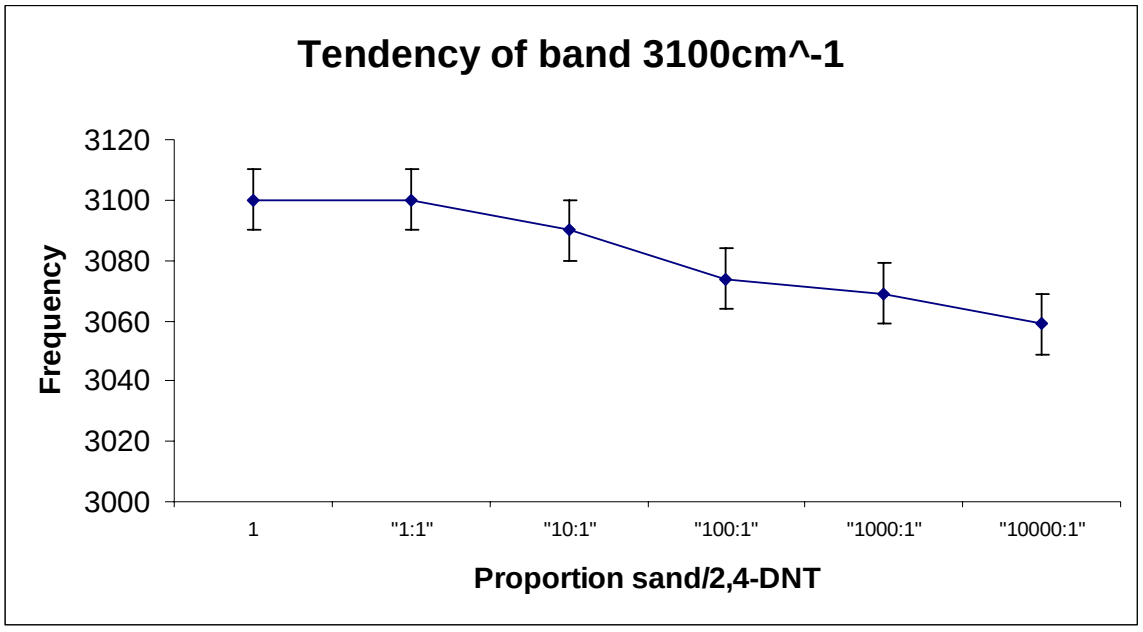

Figure 5.32 Tendency of band 3100 cm^{-1}

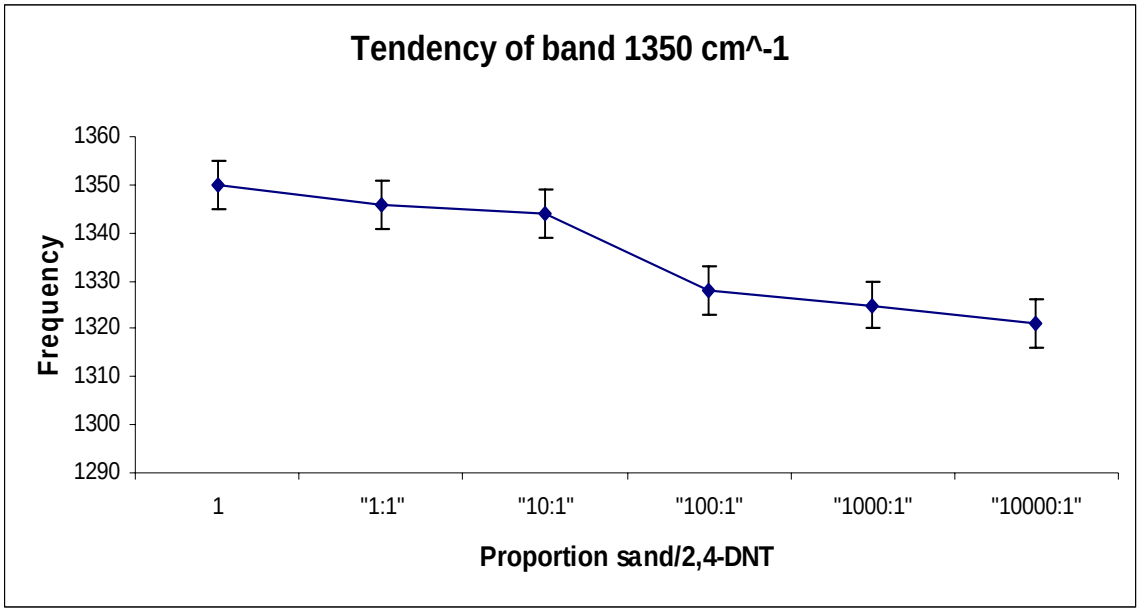

Figure 5.33 Tendency of band 1350cm^{-1}

5.3 Environmental effects on interaction 2,4-DNT/Ottawa Sand

The landmines in the field are exposed to environmental effects such as humidity, UV and temperature. In this section the results of the physical modeling of these effects measured in the laboratory are presented. These effects on mixture 2,4-DNT / Ottawa sand were based on Raman Microspectroscopy measurements.

5.3.1 Raman measurements on sand/2,4-DNT with humidity and pH

Samples of sand/2,4-DNT were placed in steel stainless cells, marked and distilled water was added in different proportions: 9%, 33% and 50% w/w. Raman spectra were then measured. Figure 5.24 shows that DNT bands taken as references such as 1350 and 1610 cm$^{-1,}$ assigned to symmetric NO_2 stretching vibration and aromatic-NO_2 conjugation showed a shift of –21 cm^{-1} return to the initial frequency. For samples in

cells at pH 4, 7, 10 Raman spectra were taken. Reference bands are also moved to their initial site showing a behavior similar to the samples in the presence of humidity [James, 2001], which are observed in the Figure 5.23.

Samples of 2,4-DNT were deposited in stainless steel cells and placed in desiccator for 6 hours to remove the humidity and the Micro Raman spectra were measured. The Raman data are shown in Figure 5.34. Spectrum (b) of sand/2,4-DNT shows a shift of these signals that points towards an interaction of sand and explosive that in the presence of water and in contact with sand at pH 4, 7 and 10 these interaction is no longer present. This effect can also be observed in several regions of the spectra (see Figure 5.35).

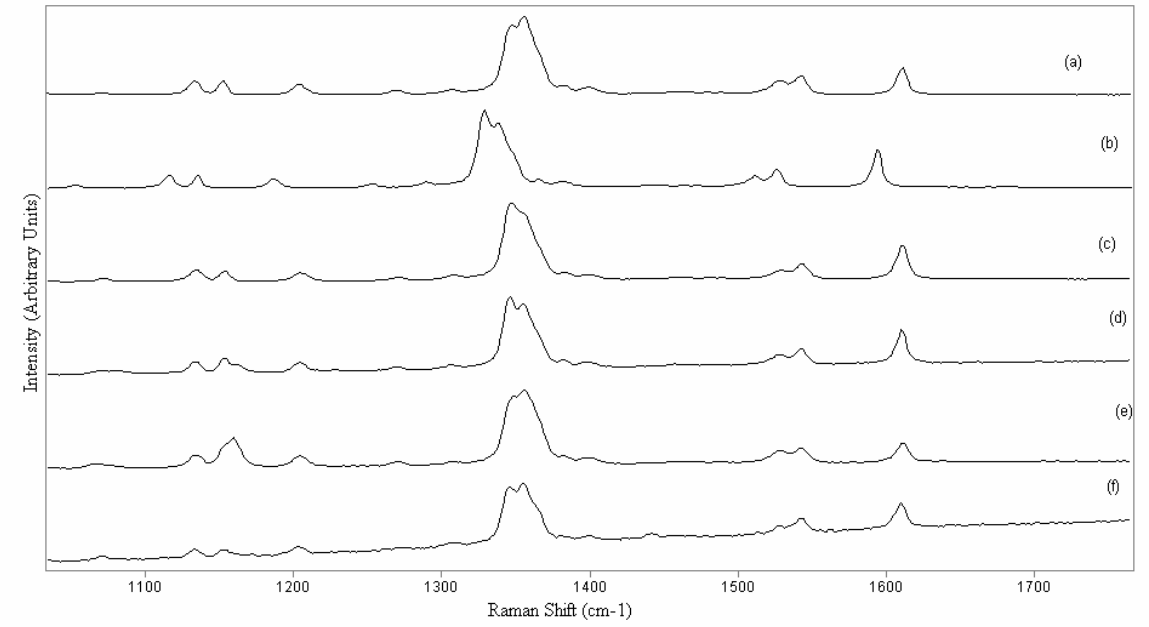

Figure 5.34. Water and pH effect on DNT-Sand mixture, NO_2 Region: (a) DNT crystals, (b) Sand/DNT Mix, (c) Mix at 9 % H_2O, (d) Mix at 33 % H_2O, (e) Mix at 50 % H_2O, (f) Mix at pH = 4.

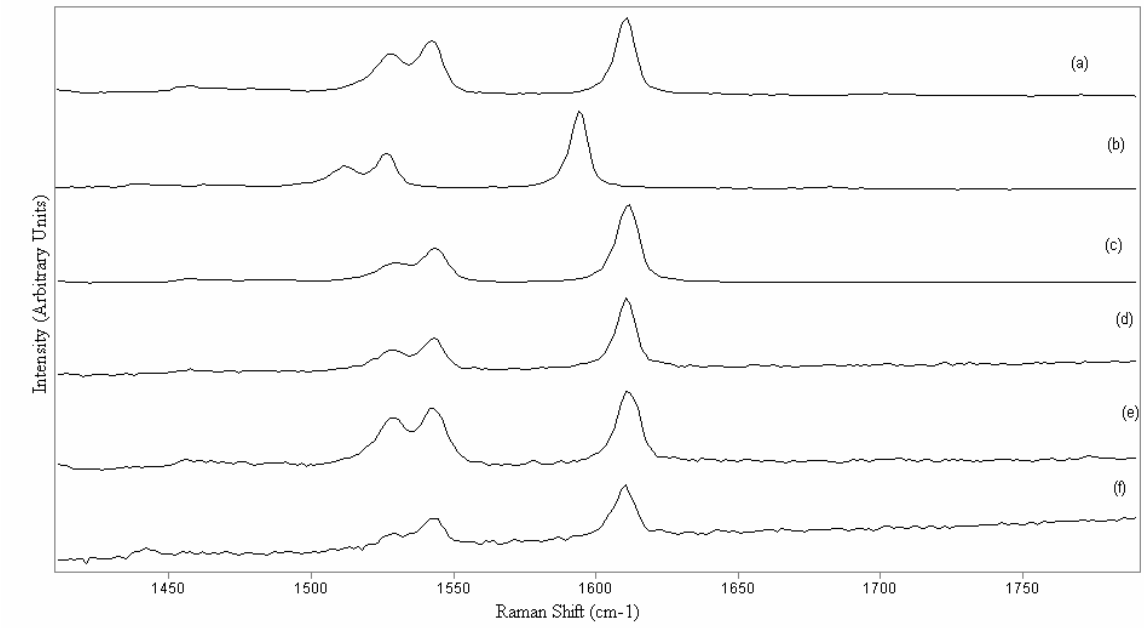

Figure 5.35 Water and pH effect on DNT-Sand mixture, Ring Signals: (a) DNT crystals, (b) Sand/DNT Mix, (c) Mix at 9 % H_2O, (d) Mix at 33 % H_2O, (e) Mix at 50 % H_2O, (f) Mix at pH = 4.

Samples were taken from the Sand/2,4-DNT mix and placed in stainless steel cells and mixed with 1M NaOH solution. The pH values were adjusted to 10, 11, 12 and 13 during 8 hours. Typical Raman spectra taken are shown in Figures 5.36-37. It can be observed that the characteristic signals of 2,4-DNT decrease in intensity until disappearing at pH 13. At pH 10 and above explosive is degraded and at pH 13 the characteristic signals of 2,4-DNT were not observed.

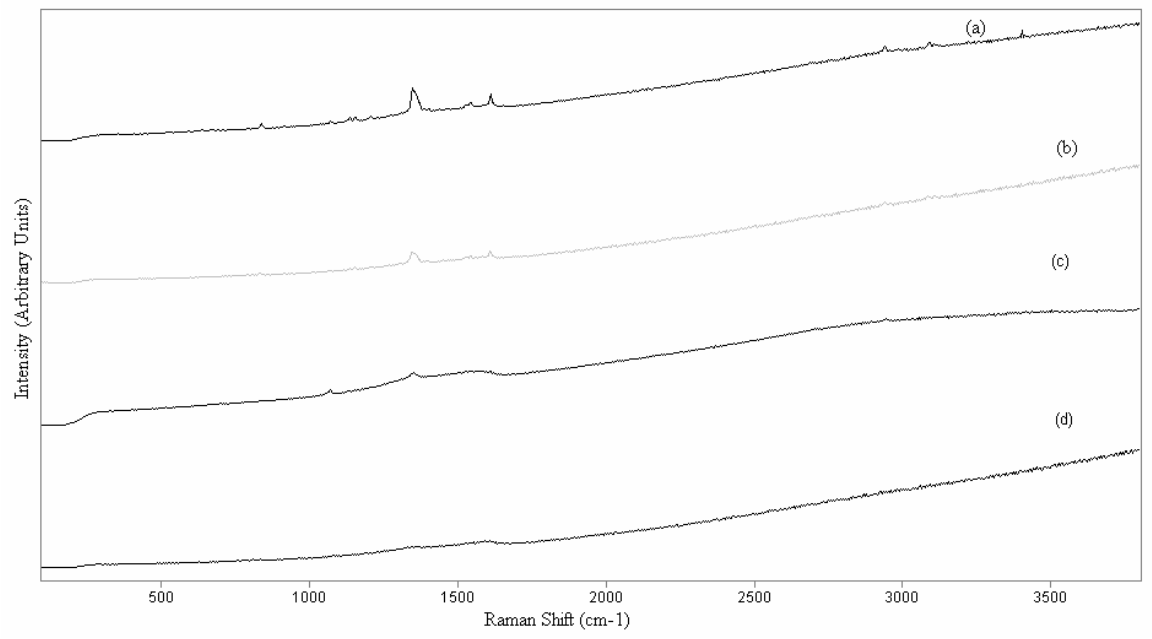

Figure 5.36 Effect of pH on DNT: (a) pH = 10, (b) pH = 11, (c) pH = 12, (d) pH = 13.

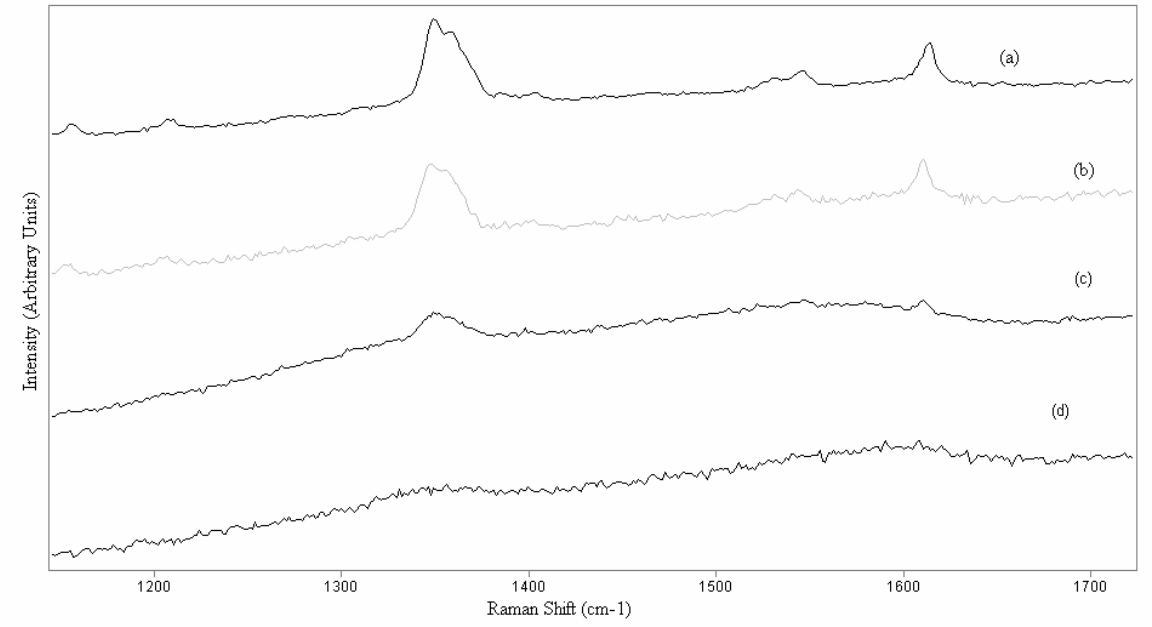

Figure 5.37 Effect of pH on DNT: (a) pH = 10, (b) pH = 11, (c) pH = 12, (d) pH = 13.

5.3.2 Raman measurements on Sand/2,4-DNT at different Temperatures.

Samples of sand/ 2,4-DNT were placed in stainless steel cells and maintained at 40, 50, 60, 70 and 80 ^{o}C. Raman spectra were analyzed in several regions from 100 to 3800 cm^{-1}. The spectroscopic window at ca. 1200-1700 cm^{-1} is shown in Figures 5.38-5.39. The characteristic signal at 1350 cm^{-1} in the different ranges from temperatures was observed over 70 ^{o}C, the intensities of 2,4-DNT signatures decreased until disappearing at 80 ^{o}C. This is indicative of the degradation of the explosive.

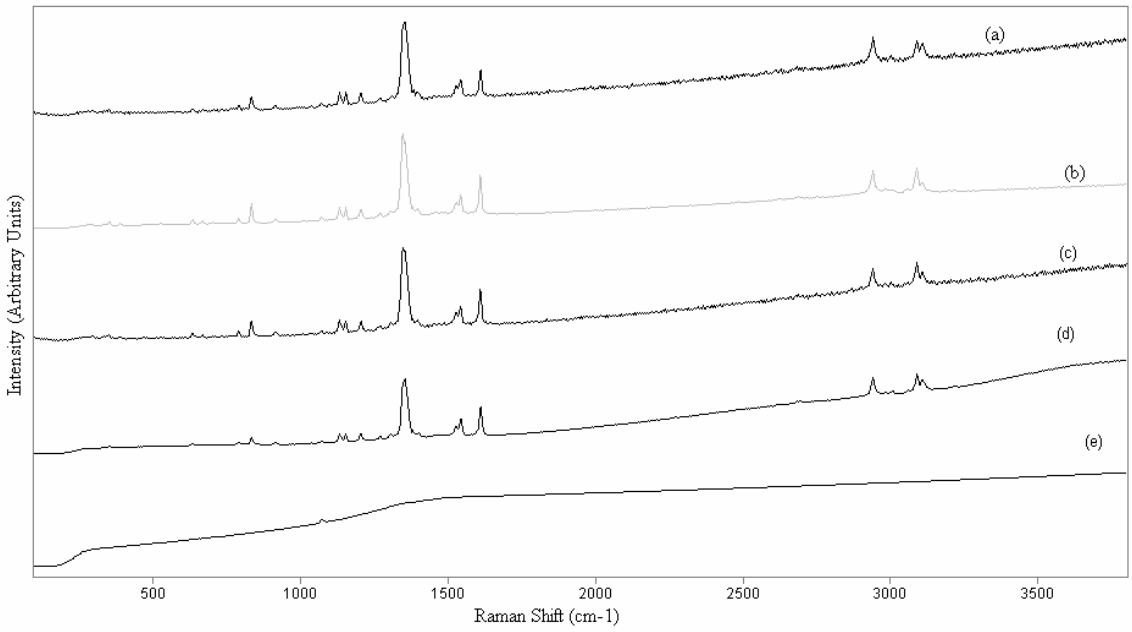

Figure 5.38. **Effect of heat on DNT Raman Signatures at 100–3600 cm^{-1} at: (a) 40 ^{o}C, (b) 50 ^{o}C, (c) 60 ^{o}C, (d) 70 ^{o}C, (e) 80 ^{o}C.**

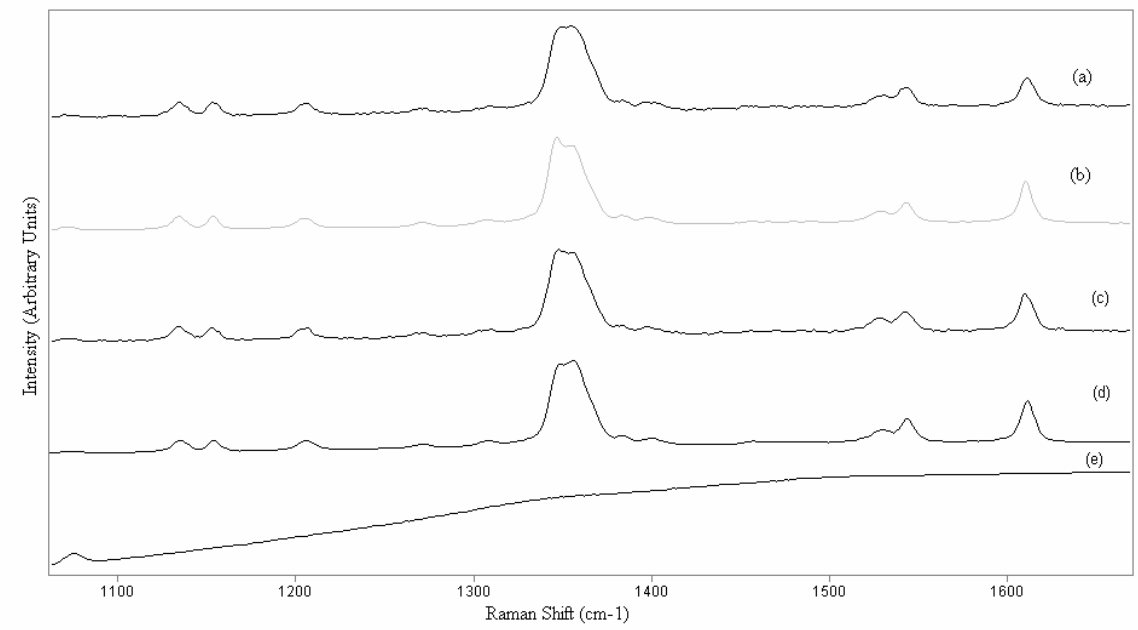

Figure 5.39 Effect of Temperature on DNT Raman Signatures at 1100 – 1700 cm^{-1}: (a) 40 °C, (b) 50 °C, (c) 60 °C, (d) 70 °C, (e) 80 °C.

5.3.3 Effect of Ultraviolet Light on 2,4-DNT.

Samples of 2,4-DNT were placed under ultraviolet light at 254 nm and Raman spectra were taken as a function of time in an interval of 24 hours for 336 h (two weeks). Characteristic signals of 2,4-DNT were analyzed in different ranges: 600-1200 cm^{-1}, 300-1700 cm^{-1} and 2800-3500cm^{-1} (Figures 5.40-5.43). The intensity of the signals was found to decrease with time. No new signals were observed that could be used to characterize possible degradation products. Some of these products could be in gaseous phase while Raman spectra were taken on the sand surface. Thus these could not be observed.

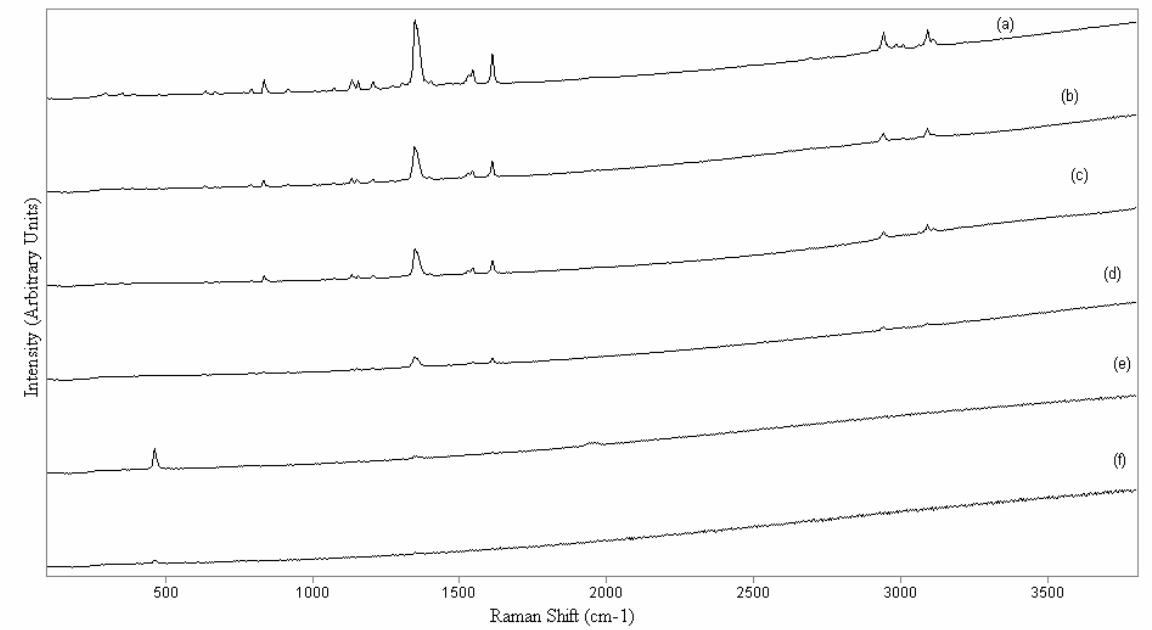

Figure 5.40 Effect of UV exposure: (a) 2,4-DNT with no UV exposure, (b) 24 h, (c) 48 h, (d) 72h, (e) 96 h, (f) 336 h.

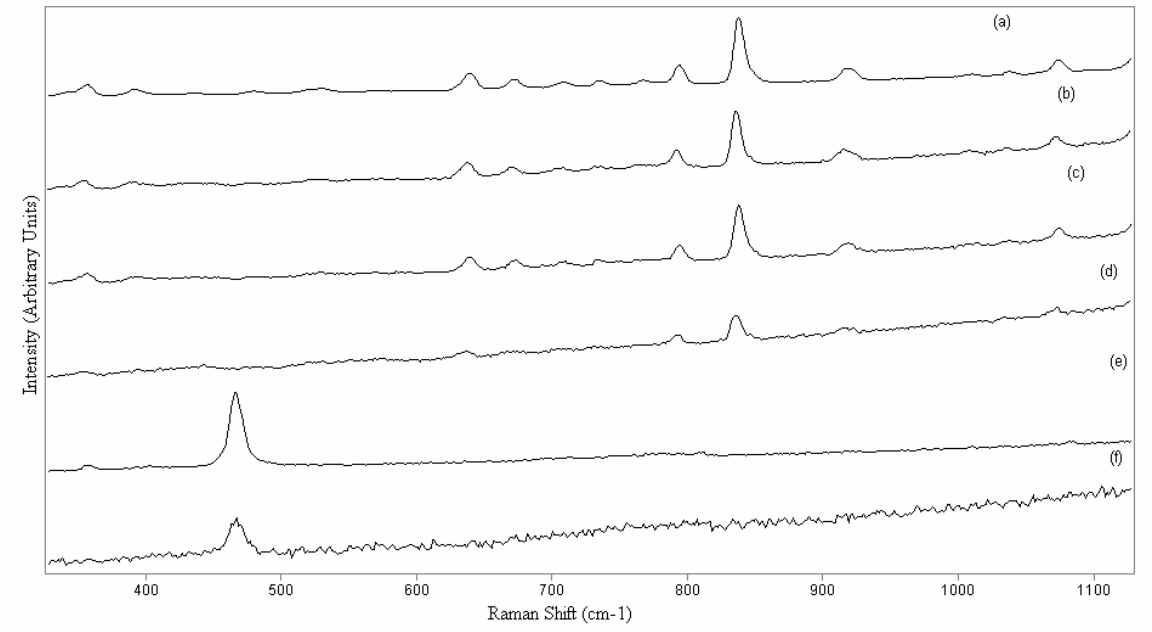

Figure 5.41 Effect of UV exposure: (a) 2,4-DNT, (b) 24 h, (c) 48 h, (d) 72 h, (e) 96 h, (f) 336 h.

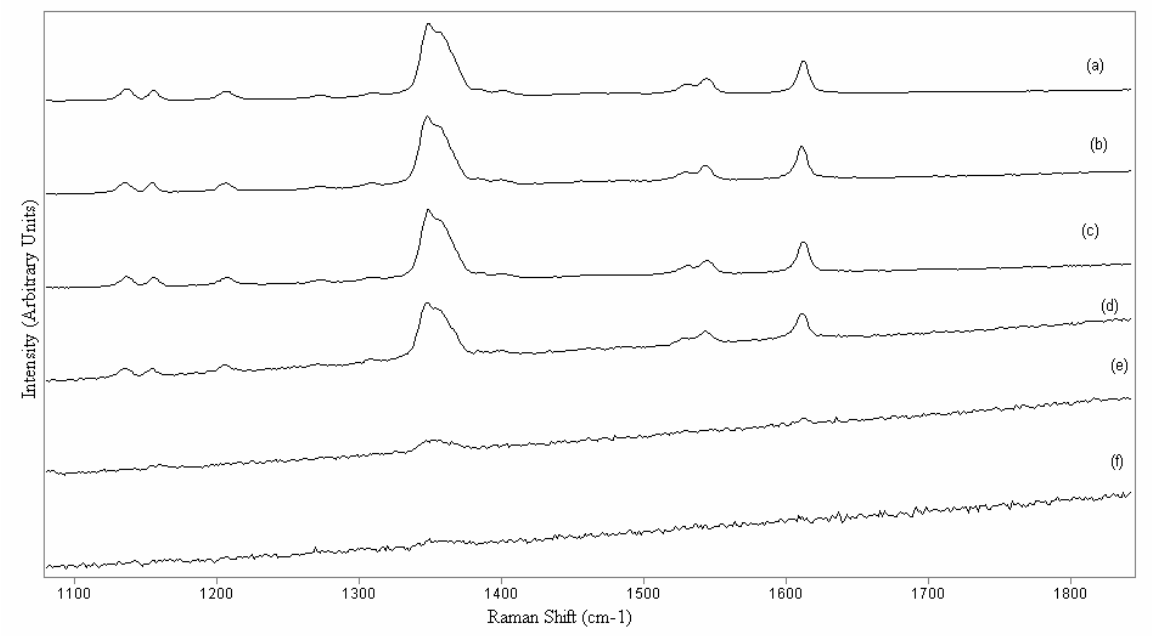

Figure 5.42 (a) 2,4-DNT, (b)24 h, (c) 4 8h, (d) 72 h, (e) 96 h, (f) 336 h.

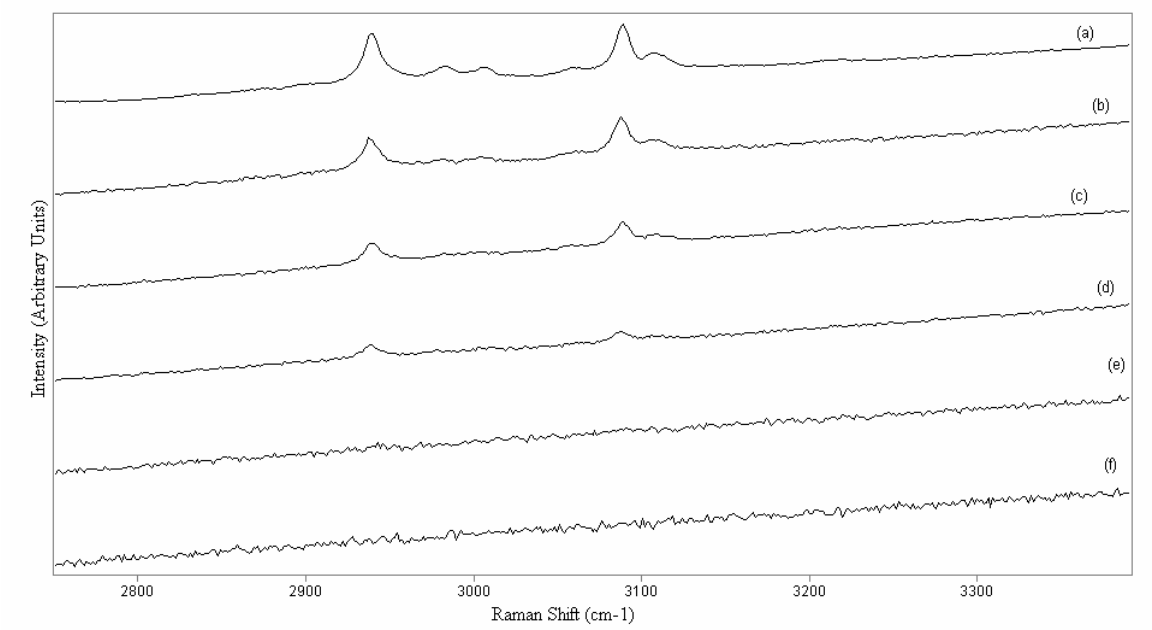

Figure 5.43 Effect UV exposure: (a) 2,4-DNT, (b) 24 h, (c) 48 h, (d) 72 h, (e) 96 h, (f) 336 h.

5.3.4 Effect of Ultraviolet light on 2,4-DNT at pH = 10 and H_2O_2.

Samples of 2,4-DNT at pH = 10 were placed in the presence of ultraviolet light and H_2O_2 during 6 hours Raman spectra were taken. Significant changes in the intensities during the first 2 hours were observed. After 2 hours, characteristic signals of 2,4-DNT decreased by the effect of ultraviolet light in the presence of H_2O_2 at pH =10 (Figures 5.44-5.46). This acceleration in the degradation can be explained by the formation of free radicals arising from H_2O_2 in the presence of ultraviolet light. It was observed in the spectra taken at 2 and 3 hours the appearance from a new band 890 cm^{-1} that could be associated with the products of degradation. These products could also be in gaseous phase making it difficult detect them using Raman Spectroscopy. Samples of mixtures were placed in glass vials for 8 hours and after were analyzed in the gaseous phase in GC by headspace by 15 minutes. This analysis is shown in Figure 5.47. The presence of 2,4-DNT was confirmed and other signals were not identified see Table 5.4. These components can be identified by GC-MS.

Table 5.4GC Retention Times (t_R)

Retention Time (min)	Explosives
6.882	2,6-DNT
7.347	Not identified (N. I)
7.794	2,4-DNT
8.284	(N. I)

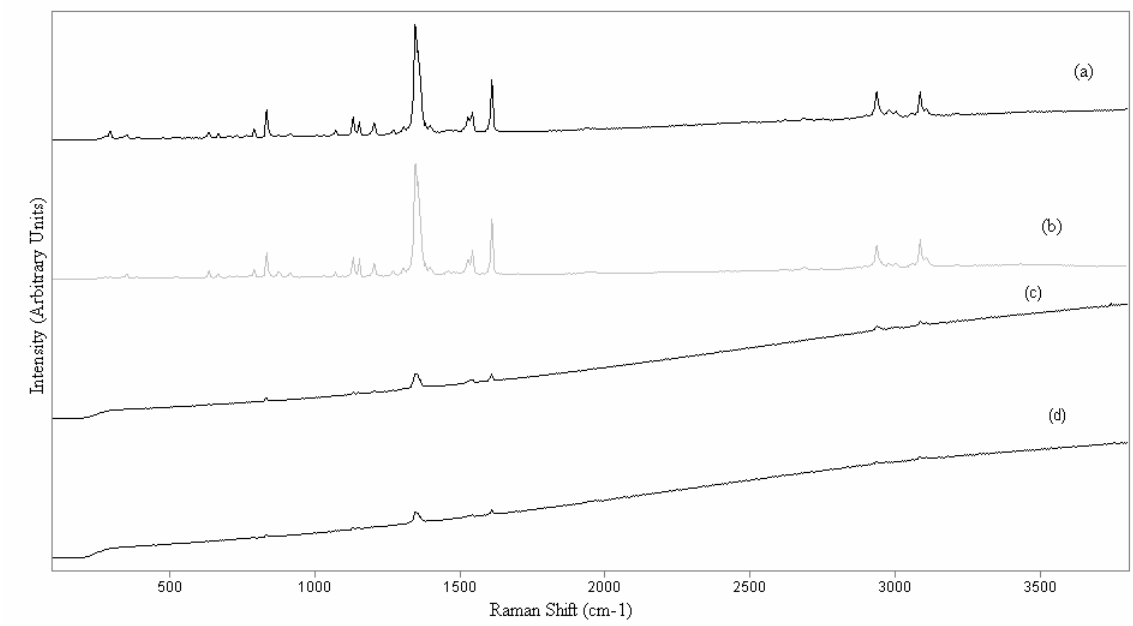

Figure 5.44 Effect of addition of H_2O_2 and alkali (pH = 10), 750-1300 cm^{-1} region: (a) Neat DNT (b) 1 h, (c) 2 h, (d) 3 h.

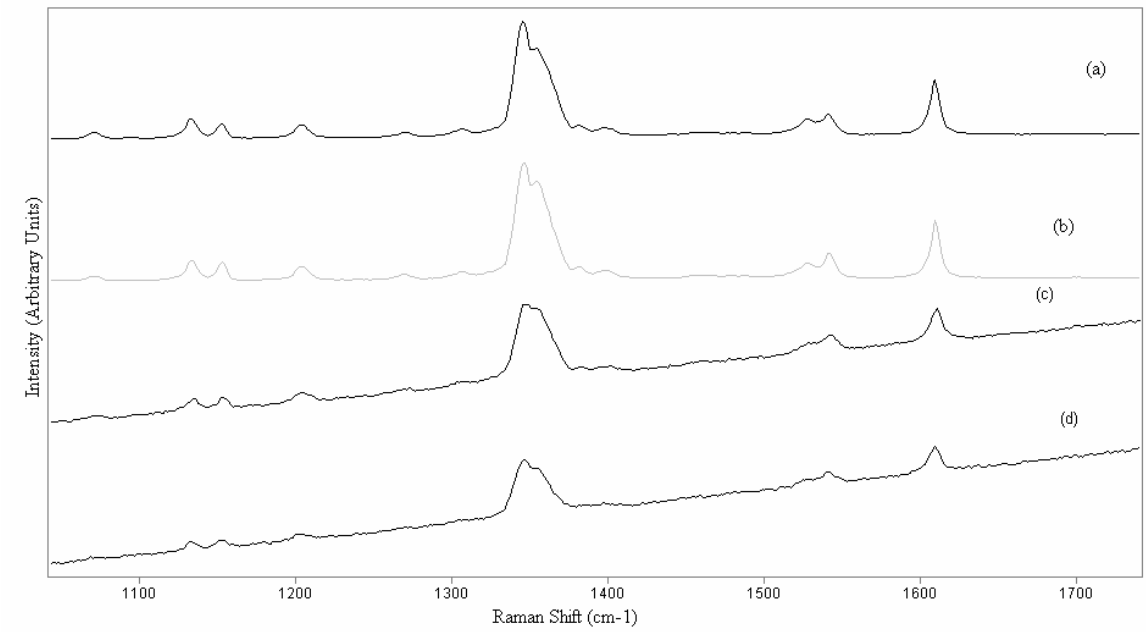

Figure 5.45 Effect of addition of H_2O_2 and alkali (pH = 10), 750-1300 cm^{-1} region: (a) Neat DNT (b) 1 h, (c) 2 h, (d) 3 h.

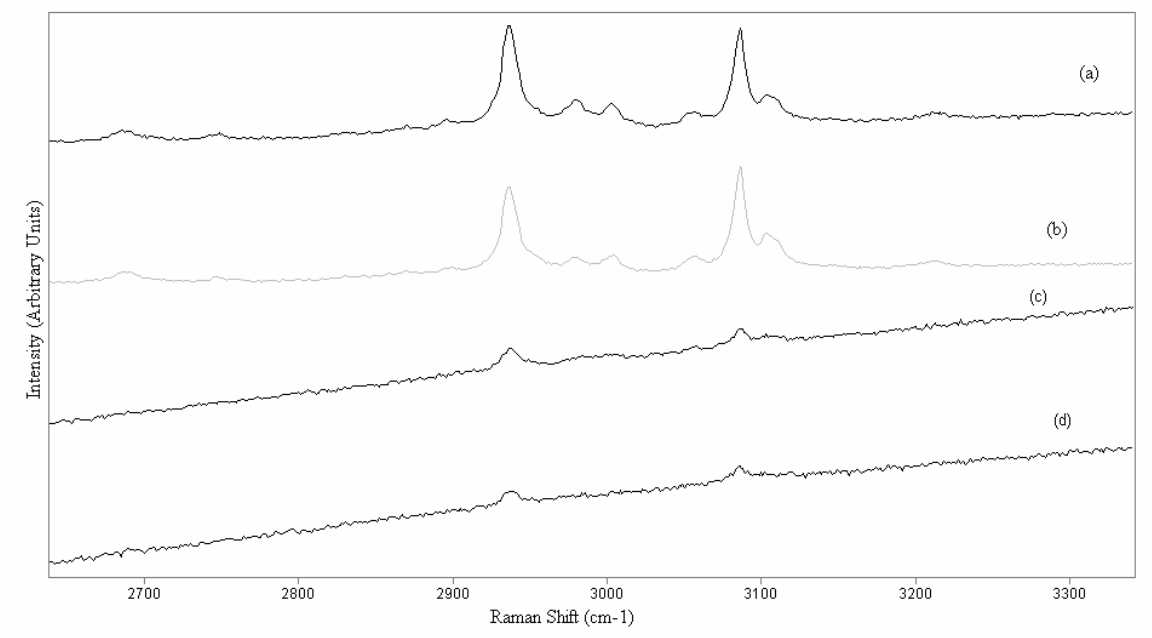

Figure 5.46 Effect of addition of H_2O_2 and alkali (pH = 10), 750-1300 cm^{-1} region: (a) Neat DNT (b) 1 h, (c) 2 h, (d) 3 h.

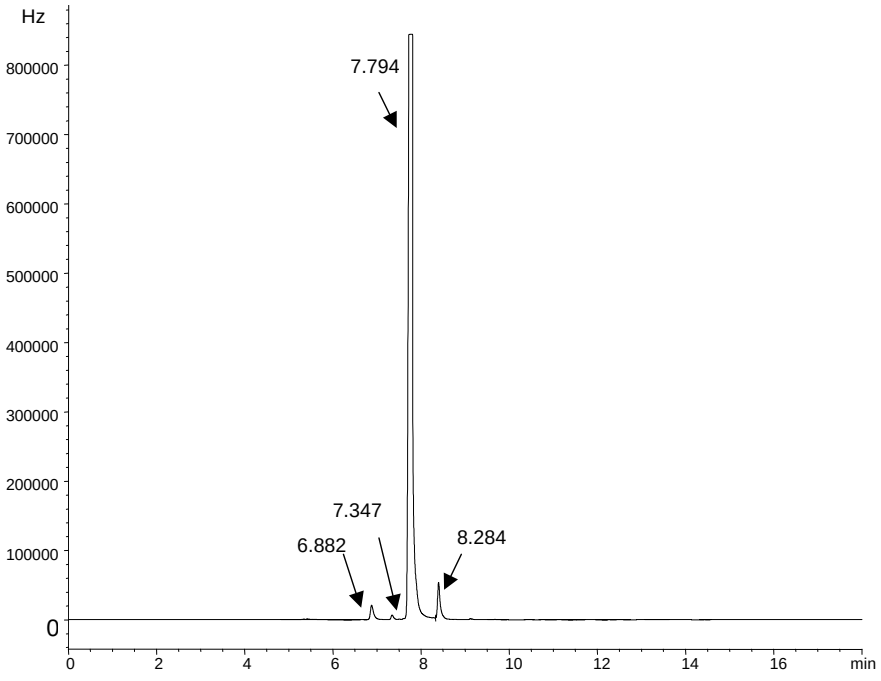

Figure 5.47 GC Analysis of gas phase products of UV irradiation of sand-DNT mixtures.

Chapter 6
Conclusions

The Raman spectra of crystals samples of 2,4-DNT obtained from micro crystallization of standard solution did not show significant changes when principal bands of crystals were compared to droplets of 2,4-DNT. However there are four bands present in crystalline samples of 2,4-DNT that did not appear in the spectra for the 2,4-DNT droplets formed by pipette transfer of DNT solutions at low concentrations (~ 5 ppm).

As a result of the Ottawa sand / explosive interaction, displacement of Raman signals were found, in the respective signatures of both components of the mixture. The maximum displacement of the Raman bands of 2,4-DNT/sand were seen in the 10000:1mixturThis effect is attributed to the fact that if A represents sand particles and B stands fro DNT, then interactions between B and A are more probable than those of B with itself.

The band that showed the largest displacement of the Raman signal was the symmetric NO_2 stretching vibration located about 1350 cm^{-1}. Nitro group with sand, the sand band at 460 cm^{-1} (deformation out plane of SiOH) showed a low frequency shift . This is the band of sand that possible has a interaction with 2,4- DNT.

Raman spectroscopy is a powerful tool to observe 2,4-DNT in sand. The low level of detection of DNT could be less than the one obtained of 10000:1, because the characteristic signal of 2,4-DNT has good intensity and could be detected to higher

proportion. However, higher mixing ratios were difficult to prepare in homogeneous mixtures.

Water and pH fixing solutions at values between 4 and 10 appear to break the interaction between sand and 2,4-DNT and do not affect the characteristic signals of the pure explosive. No significant shifting of Raman signatures of DNT was observed during the experiments. At pH values of 10 and above the characteristic signals of 2,4-DNT show degradation and pH 13 are fully degraded.

At temperatures of 70 ^{o} C and higher the signals of 2,4-DNT diminish in intensity until disappearing at 80 ^{o}C. This could be indicative of degradation of the explosive. The intensity of the signals under ultraviolet light decreased with time. No new signals that could be attributed to degradation products were observed. The presence of UV light accelerates the degradation of DNT.

Chapter 7
Future Work

Further work is recommended to further confirm the interaction of 2,4-DNT with sand. Both Raman and infrared spectroscopies should be used as well as surface analysis techniques. In the area of explosives detection, work could be done in the field using Raman portable with fiber optic coupled Raman Spectrometers.

Another recommendation is to work on the development a new method of detection increasing the Raman signal from DNT such as Surface Enhanced Raman Scattering in one or more of its many variations. Raman and infrared vibrational imaging should also be done to monitor the surfaces of the mixtures.

In the case of detection of degradation products, chromatography would contribute to characterize the UV and thermally induced degradation of nitroaromatic explosives. Gas chromatography would be used to account for emerging vapors and for volatile products. In the case of non-volatile compounds produced, high performance liquid chromatography (HPLC) would be useful for separation and characterization.

References

Akhavan, J. *The Chemistry of Explosives*, 1st ed.; The Royal Society of Chemistry: Massachusetts, 1998; pp 45-60.

Blanco, A.; Mina, N.; Castro, M.; Castillo, J.; Hernandez- Rivera, S. Spectroscopic characterization of nitroaromatic landmine explosives. *SPIE Defense & Security Symposium.* **2004**, Vol 5415**.**

Brannon, J.M**.**; Pennington, J.; *U.S. Army Engineers Research and Development Center.* Annual report 2002.

Bruschini, C.; De Bruyn, K.; Salí, H.; Cornelis, J.; *Study on the state of the art in the EU related humanitarian demining technology, product and practice*. Annual report, 1999.

Buttner, M.; Findlay, W.; Davis, M. In situ detection of dinitrotoluene and other nitrated explosives in soils. *Analytica Chimica Acta* **1997**, 63-71.

Clarke, R.H.; Londhe, S.; Premasiri, W.R.;Womble, M.E. Low-Resolution Raman Spectroscopy: Instrumentation and Applications in Chemical Analysis. *J. Raman Spectrosc*. **1999**, 30, 827–832.

Clarkson, J.; Smith, W.E.; Batchelder, D.N.; Smith, D.A.; Coats, A.M. A theoretical study of the structure and vibrations of 2,4,6-trinitrotoluene. *J. Molec. Struct.* **2003,** 648, 203-214.

Federoff, B.T. *Encyclopedia of Explosives and Related Items.* Dover, New Jersey, pp. T259-T264,1980.

Ferraro**,** J.R.; Nakamoto, K. *Introductory Raman Spectroscopy*. Academic Press, California, 1994, pp 13-26.

Fisher M.; Cumming C.; Fox, M.; LaGrone, M.; Jacob, S.; Reust, D.; Rockley, M.; Towers, E. *Nomadics Inc. white papers.* Annual report, 2000.

George V.; Jenkins, T.F.; Leggart, D.C.; Cragin, J.H. *Proceedings of SPIE* 3710, 258, SPIE. Bellingham, WA,1999.

Glenn, R.; Johnson**;** Rakesh, K.; Jain, Jim. Origins of the 2,4-Dinitrotoluene Pathway Air Force, *Research Laboratory*, U.S. Air Force, 32403, 2002.

Gupta, N.; Dahmani, R. AOTF Raman spectrometer for remote detection of explosives. *Spectrochim. Acta Part A*, **2000**, 56, 1453-1456.

Jacqueline; MacDonald, J.R.; Lockwood; McFee, J.; Altshuler, T.; Broach, T.; Carin, L.; Harmon, R.;Carey, R.; Scott, W.; Weaver, R. Detection alternatives landmine detection. Science and Technology Policy Institute Prepared for the Office of Science and Technology Policy, 2003.

James, S.; James, A. J.; Klein, J.D.; Kevin, M.; Spencer. Surface-Enhanced Raman Detection of 2,4-Dinitrotoluene Impurity Vapor as a Marker To Locate Landmines. *Anal. Chem*.**2000**, 72, 5834-5840.

James, P.; James, L. Solubility of 2,4-Dinitrotoluene and 2,4,6-Trinitrotoluene in Water. *J. Chem. Eng. Data* **2001**, 46, 375-376.

Katrin, K.; Kneipp, H.; Itzkan, I.; Ramachandra, R.; Feld, M.S. Ultrasensitive Chemical Analysis by Raman Spectroscopy. *Chem Rev.* **1999**, 99, 2957-2975

Kenna, B.T.; Conrad F.J. *Sandia Report* SAND86-0141, Sandia National Laboratories, 1986.

Lewis, R.; Siems, N.W.; Daniel, P.T. *Applied Spectroscopy,* **1997** 51, 1854.

Lynch, K. F.; Myers, J.M.; Brannon, J.J. Effects of pH and Temperature on the Aqueous solubility and Dissolution Rate of 2, 4, 6 - Trinitrotoluene and HMX. *J.Chem.Eng .Data.* **2001**, 46, 1549-1555.

McCreery, R.L. *Raman Spectroscopy for Chemical Analysis*. John Wiley & Sons, New York, 2000; pp 326-327.

McCrone, W.C. Solubility, Recrystalization and Microchemical Tests on Nanogram Single Particles. *Microscopy*, **1998**, 86,107-118.

Naal, J.H.; Abruna, H.D. Amperometric TNT Biosensor Based on the oriented Immobilization of a Nitroreductase Maltose Binding Protein Fusion. *Anal. Chem*. 2002, 74, 140-148.

Nolan, R.; Gravite, D. *Report 2217*, US Army Mobility Research and Development Command, 1977.

Ortega, C.; Fresh, H. H. Biodegradation of sorbed 2,4-dinitrotoluene in a Clay-Rich, Aggregated porous medium. *Environ. Sci Technol.* **1999**, 33, 3737-3742.

Paul, R.G.; Holt, D.B.; Lake, L.S. Explosives detection in soil using a field-portable continuous flow immunosensor. *Journal of Hazardous Materials*. 200183, 51-63.

Silverstein, R.M.; Webster, F.X. *Spectrometric Identification of Organic Compounds.* John Wiley & Sons, New York, 1998.

Thorn, P.G.; Thorne; Cox, L.G. Alkaline Hydrolysis/Polyremerization of 2,4,6-Trinitrotoluene, Characterization of products by C^{13} and N^{15} NMR. *Environ. Sci. Technol.* **2004**, 38, 2224-2231.

Yinon, J. *Forensic and environmental detection of explosives,* John Wiley & Sons, LTD, England, 1999; chapter 6.